Research Square

Preprints are preliminary reports that have not undergone peer review.
They should not be considered conclusive, used to inform clinical practice,
or referenced by the media as validated information.

Mathematical Assessment of Three-Year Field Performance and Growth Promotion Efficiency of Bacillus pumilus and Bacillus thuringiensis in Brassica juncea

Shambhu Swarnakar
Raiganj University
Papan Chowhan
Raiganj University
Sumi Paul
Raiganj University
Arka Pratim Chakraborty
arka.botanyrgu@gmail.com
Raiganj University

Research Article

Keywords: Brassica juncea, Bacillus pumilus, Bacillus thuringiensis, Plant growth-promoting rhizobacteria (PGPR), Fusarium equiseti, Induced systemic resistance (ISR), biological control, three-year field evaluation, mathematical assessment, growth promotion, GC–MS, and sustainable agriculture

Posted Date: August 15th, 2026

DOI: https://doi.org/10.21203/rs.3.rs-10577055/v1

License: This work is licensed under a Creative Commons Attribution 4.0 International License.
Read Full License

Additional Declarations: No competing interests reported.

Mathematical Assessment of Three-Year Field Performance and Growth Promotion Efficiency of *Bacillus pumilus* and *Bacillus thuringiensis* in *Brassica juncea*

Shambhu Swarnakar[1], Papan Chowhan[1], Sumi Paul[1], Arka Pratim Chakraborty[2]*
1. Research Scholar, Department of Botany, Raiganj University, Uttar Dinajpur–733134, West Bengal, India
2 Assistant Professor, Department of Botany, Raiganj University, Uttar Dinajpur–733134, West Bengal, India.*

*Corresponding author: arka.botanyrgu@gmail.com

Abstract

Yellow leaf disease caused by *Fusarium equiseti* has emerged as a serious constraint to mustard (*Brassica juncea* L.) production, resulting in substantial reductions in plant growth and yield. The present study aimed to identify the causal pathogen of yellow leaf disease and evaluate the plant growth-promoting, biocontrol, and induced systemic resistance (ISR) potential of two rhizospheric bacterial isolates. Diseased mustard leaves collected from Uttar Dinajpur district, West Bengal, India, yielded a fungal isolate (MUSLD-01), which was identified as *Fusarium equiseti* through morphological, scanning electron microscopic, and molecular analyses. Two rhizospheric bacterial isolates were identified as *Bacillus pumilus* (GenBank accession ON783696) and *Bacillus thuringiensis* (GenBank accession OQ415951) based on 16S rDNA sequencing. Both isolates exhibited multiple plant growth-promoting traits, including indole-3-acetic acid production, phosphate solubilization, siderophore production, and catalase activity. In vitro dual culture assays demonstrated pronounced antagonistic activity against *F. equiseti*, with *B. thuringiensis* exhibiting comparatively greater inhibition of mycelial growth. GC–MS analysis of ethyl acetate extracts of bacterial culture filtrates revealed diverse antifungal bioactive metabolites associated with pathogen suppression. A three-year field evaluation (2023–24 to 2025–26) involving three mustard varieties (B-9, B-54, and NYC) demonstrated consistent improvements in plant height, leaf length, root length, and seed yield following PGPR inoculation. Among the tested treatments, *B. pumilus* produced the greatest growth promotion and yield enhancement, while both bacterial isolates substantially reduced the adverse effects of *F. equiseti* under field conditions.

Mathematical assessment of growth response indicated approximately 19–20% improvement in vegetative growth, 34–36% enhancement in seed yield, and about 31–33% greater root development in PGPR-treated plants compared with untreated controls. Enhanced activities of phenylalanine ammonia-lyase, peroxidase, chitinase, and β-1,3-glucanase further confirmed activation of induced systemic resistance. Collectively, the integration of microbiological, biochemical, mathematical, and multi-year field evidence demonstrates that *B. pumilus* and *B. thuringiensis* are promising eco-friendly biocontrol agents and plant growth-promoting rhizobacteria for the sustainable management of mustard yellow leaf disease and improvement of crop productivity.

Keywords

Brassica juncea; *Bacillus pumilus*; *Bacillus thuringiensis*; Plant growth-promoting rhizobacteria (PGPR); *Fusarium equiseti*; Induced systemic resistance (ISR), biological control, three-year field evaluation, mathematical assessment, growth promotion, GC–MS, and sustainable agriculture

1 Introduction

Mustard (*Brassica juncea* L.) is one of the most important oilseed crops cultivated worldwide and constitutes a major source of edible oil, protein-rich seed meal, and industrial raw materials. India is among the largest producers of mustard, where the crop plays a vital role in ensuring edible oil security and supporting the livelihood of millions of farmers. Despite continuous improvements in agronomic practices and varietal development, mustard productivity remains considerably below its genetic potential due to various biotic and abiotic stresses. Among the biotic constraints, fungal diseases are responsible for substantial reductions in plant growth, seed quality, and yield. Yellow leaf disease has recently emerged as an important disease affecting mustard cultivation in several regions of eastern India. The disease is characterized by progressive chlorosis along leaf margins and veins, premature senescence, reduced photosynthetic efficiency, stunted growth, and significant yield losses. As the disease progresses, infected plants exhibit reduced vigor and poor

seed development, leading to considerable economic losses. Although several fungal pathogens have been associated with foliar diseases of mustard, increasing evidence suggests that *Fusarium equiseti* has become an important causal agent of yellow leaf symptoms under favorable environmental conditions.

Species belonging to the genus *Fusarium* are widely distributed soil-borne fungi capable of infecting a broad range of economically important crops. Besides causing vascular wilt, root rot, damping-off, and seedling blight, several *Fusarium* species produce mycotoxins that adversely affect crop quality and food safety. *Fusarium equiseti*, traditionally regarded as an opportunistic pathogen, has recently attracted considerable attention because of its increasing association with foliar diseases in oilseed and vegetable crops. The persistence of fungal propagules in soil and crop residues, together with their adaptability to diverse environmental conditions, makes disease management particularly challenging. Management of *Fusarium*-associated diseases largely depends on synthetic fungicides. However, prolonged and indiscriminate application of chemical pesticides has resulted in environmental contamination, disruption of beneficial soil microbiota, accumulation of toxic residues, and the emergence of fungicide-resistant pathogen populations. These limitations have stimulated increasing interest in environmentally sustainable disease management strategies that minimize chemical inputs while maintaining crop productivity.

Plant growth-promoting rhizobacteria (PGPR) have emerged as one of the most promising biological alternatives for sustainable crop protection. These beneficial microorganisms colonize the rhizosphere and enhance plant growth through multiple direct and indirect mechanisms, including biological nitrogen fixation, phosphate solubilization, production of phytohormones such as indole-3-acetic acid (IAA), synthesis of siderophores, secretion of hydrolytic enzymes, and modulation of plant hormonal balance. In addition to promoting plant growth, PGPR suppress plant pathogens through antibiosis, nutrient competition, production of volatile organic compounds, lipopeptides, and antimicrobial metabolites, as well as activation of induced systemic resistance (ISR), thereby enhancing the plant's innate defense system.

Among PGPR, species of the genus *Bacillus* have attracted particular attention because of their exceptional ecological adaptability, endospore-forming ability, prolonged shelf life, and capacity to produce a diverse array of antimicrobial secondary metabolites. *Bacillus pumilus* and *Bacillus*

thuringiensis have been reported to exhibit strong antagonistic activity against several phytopathogenic fungi while simultaneously promoting plant growth and improving tolerance to biotic and abiotic stresses. Their ability to produce lipopeptides, siderophores, hydrolytic enzymes, antibiotics, and phytohormones makes them attractive candidates for the development of eco-friendly bioinoculants. Although numerous studies have reported the growth-promoting properties of PGPR under controlled conditions, relatively few investigations have integrated pathogen identification, biochemical characterization, metabolite profiling, induced defense responses, and long-term field validation against *Fusarium equiseti* in mustard. Furthermore, quantitative mathematical assessment of plant growth responses across multiple growing seasons remains scarce, limiting our understanding of the consistency and practical applicability of PGPR under natural field environments.

Therefore, the objectives of the present investigation were to (i) isolate and identify the causal agent of yellow leaf disease of mustard; (ii) characterize rhizospheric isolates of *Bacillus pumilus* and *Bacillus thuringiensis* for their plant growth-promoting and antagonistic properties; (iii) identify antifungal metabolites using GC–MS analysis; (iv) evaluate their ability to induce systemic resistance through defense-related enzymes; (v) assess their efficacy in suppressing *Fusarium equiseti* and promoting plant growth during a three-year field evaluation involving three mustard varieties; and (vi) perform a mathematical assessment of growth promotion and yield enhancement to quantify the long-term effectiveness and stability of these PGPR under field conditions. The findings provide comprehensive evidence supporting the development of *B. pumilus* and *B. thuringiensis* as sustainable bioinoculants for the eco-friendly management of mustard yellow leaf disease.

2 Materials and Methods

2.1 Survey and sample collection

A systematic field survey was conducted during three consecutive rabi (winter) cropping seasons (2023–24, 2024–25, and 2025–26) in major mustard-growing areas of Khowaspur village,

Karandighi Block, Uttar Dinajpur District, West Bengal, India, to assess the occurrence and distribution of yellow leaf disease in *Brassica juncea*. Surveys were performed from November to February each year, corresponding to the active vegetative and reproductive growth stages of the crop.

Prior permission was obtained from the concerned landowner(s) before conducting the field survey and collecting soil and plant samples at Khowaspur village. The field sampling was conducted solely for academic and research purposes.

Five representative mustard fields were selected based on cropping intensity and disease occurrence. Plants exhibiting typical yellow leaf disease symptoms, including chlorosis along the leaf margins and midrib, interveinal yellowing, premature senescence, and reduced plant vigor, were randomly sampled following standard phytopathological survey procedures. Approximately 20–25 symptomatic plants were examined in each field, and representative infected leaves were collected aseptically in sterile polyethylene bags to prevent contamination during transport.

The geographical coordinates of each sampling site were recorded using a handheld Global Positioning System (GPS) receiver. Field observations, including disease incidence, symptom severity, crop growth stage, and environmental conditions, were documented during each survey. The collected samples were transported to the Plant Pathology Laboratory, Department of Botany, Raiganj University, and processed within 24 h for pathogen isolation and identification. Survey locations, geographical coordinates, and major disease symptoms observed during the investigation are presented in Table 1.

Table 1. Survey locations and disease incidence of yellow leaf disease of *Brassica juncea* in Uttar Dinajpur District, West Bengal, India.

Location	Block	District	GPS coordinates	Disease incidence (%)	Predominant symptoms
Khowaspur	Karandighi	Uttar Dinajpur	25.772671° N, 88.032848° E	42.6	Yellowing along leaf margins and midrib, interveinal chlorosis, premature senescence

2.2 Isolation and identification of the fungal pathogen

Leaf samples exhibiting characteristic yellow leaf disease symptoms were processed immediately after collection for fungal isolation. Infected leaf tissues (approximately 5 × 5 mm), excised from the advancing margins of lesions, were washed thoroughly under running tap water and surface sterilized by immersion in 70% ethanol for 30 s, followed by 1% sodium hypochlorite solution for 1–2 min, and finally rinsed three times with sterile distilled water. The sterilized tissue pieces were blotted dry on sterile filter paper and aseptically transferred onto potato dextrose agar (PDA) medium supplemented with an appropriate antibacterial antibiotic to suppress bacterial contamination. The inoculated plates were incubated at **25 ± 2 °C** for **7–10 days** under a **12 h light/12 h dark photoperiod**.

Emerging fungal colonies were purified by the hyphal tip method and maintained on fresh PDA slants for subsequent investigations. A representative isolate, designated **MUSLD-01**, was selected based on colony morphology and disease association. Macroscopic characteristics, including colony color, texture, pigmentation, and growth pattern, were recorded after seven days of incubation. Microscopic observations were performed using a compound light microscope to examine hyphal morphology, septation, conidiophore structure, and macroconidial characteristics following standard mycological procedures.

For ultrastructural characterization, infected leaf tissues and fungal cultures were examined using scanning electron microscopy (SEM) to visualize fungal colonization and surface morphology. Transmission electron microscopy (TEM) was employed to investigate ultrastructural alterations in infected host tissues and pathogen–host interactions at the cellular level.

Genomic DNA was extracted from actively growing mycelia using a fungal genomic DNA extraction protocol. The internal transcribed spacer (ITS1–5.8S–ITS2) region of the ribosomal DNA was amplified by polymerase chain reaction (PCR) using universal fungal primers ITS1 and ITS4. PCR products were purified, sequenced, and compared with sequences available in the National Center for Biotechnology Information (NCBI) GenBank database using the BLAST algorithm for molecular identification. The nucleotide sequence of isolate MUSLD-01 was deposited in GenBank under accession number **ON783721**, confirming its identity as *Fusarium*

equiseti. Morphological and molecular characteristics of the fungal isolate are summarized in Table 2.

Table 2. Morphological and molecular characteristics of fungal isolate MUSLD-01.

Parameter	Observation
Isolate code	MUSLD-01
Culture medium	Potato dextrose agar (PDA)
Incubation temperature	25 ± 2 °C
Colony color	Whitish to pale pink with abundant aerial mycelium
Colony texture	Cottony to floccose
Hyphae	Hyaline, septate, and branched
Macroconidia	Typical *Fusarium*-type, multicellular, slightly curved
Microconidia	Present, hyaline, oval to ellipsoidal
SEM observation	Dense mycelial network with abundant conidial development
TEM observation	Extensive fungal colonization and ultrastructural damage in infected leaf tissues
Molecular marker	ITS1–5.8S–ITS2 rDNA
Molecular identification	*Fusarium equiseti*
GenBank accession number	ON783721

2.3 Isolation and characterization of plant growth-promoting rhizobacteria (PGPR)

Rhizospheric soil samples were collected from the root zones (0–15 cm depth) of healthy mustard (*Brassica juncea* L.) plants growing in disease-free areas of Khowaspur village, Karandighi Block, Uttar Dinajpur, West Bengal, India. Approximately 10 g of rhizospheric soil adhering to the roots was aseptically collected using sterile spatulas, transferred into sterile polyethylene bags, transported to the laboratory under refrigerated conditions, and processed within 24 h of collection. Bacterial isolates were obtained using the standard serial dilution plate technique. Briefly, 1 g of rhizospheric soil was suspended in 9 mL of sterile physiological saline (0.85% NaCl), serially diluted up to 10^{-6}, and 100 µL aliquots from appropriate dilutions were spread onto Nutrient Agar (NA) medium supplemented with kanamycin (50 µg mL^{-1}) to suppress non-target microbial

growth. Plates were incubated at **30 ± 2 °C** for **24–48 h**, after which morphologically distinct bacterial colonies were selected and purified by repeated streaking on fresh nutrient agar plates. Pure cultures were maintained on nutrient agar slants at 4 °C for further characterization.

Purified bacterial isolates were screened for important plant growth-promoting (PGP) traits using standard microbiological and biochemical assays. Indole-3-acetic acid (IAA) production was determined using Salkowski's reagent following growth in L-tryptophan-amended nutrient broth. Phosphate-solubilizing ability was evaluated on Pikovskaya's agar by measuring the formation of clear halo zones surrounding bacterial colonies. Siderophore production was assessed using Chrome Azurol S (CAS) agar medium, while catalase activity was determined by observing oxygen bubble formation following the addition of 3% hydrogen peroxide. Selected isolates were further examined for additional biochemical characteristics, including starch hydrolysis, protease activity, chitinase production, and hydrogen cyanide (HCN) production, following standard microbiological protocols. Based on their superior plant growth-promoting characteristics and antagonistic activity against *Fusarium equiseti*, two representative isolates were selected for molecular identification. Genomic DNA was extracted from actively growing bacterial cultures, and the nearly full-length 16S rRNA gene was amplified using universal bacterial primers 27F and 1492R. Purified PCR products were sequenced commercially, and the obtained nucleotide sequences were compared with reference sequences available in the National Center for Biotechnology Information (NCBI) GenBank database using the BLAST algorithm. Phylogenetic analysis confirmed the identity of the isolates as *Bacillus pumilus* (GenBank accession **ON783696**) and *Bacillus thuringiensis* (GenBank accession **OQ415951**). These isolates were subsequently used for all in vitro antagonistic assays, GC–MS metabolite profiling, greenhouse evaluations, and three-year field experiments.

Table 3. Morphological, biochemical, and molecular characteristics of the selected PGPR isolates.

Parameter	**Isolate me.**	**Isolate II**
Isolate code	MUSRH-05	MUSRH-08
Molecular identification	*Bacillus pumilus*	*Bacillus thuringiensis*
GenBank accession number	ON783696	OQ415951

Parameter	Isolate me.	Isolate II
Gram reaction	Positive	Positive
Cell morphology	Rod-shaped	Rod-shaped
Endospore formation	Positive	Positive
Catalase activity	Positive	Positive
Indole-3-acetic acid (IAA) production	Positive	Positive
Phosphate solubilization	Positive	Positive
Siderophore production	Positive	Positive
Chitinase activity	Positive	Positive
Protease activity	Positive	Positive
Starch hydrolysis	Positive	Positive
Hydrogen cyanide (HCN) production	Positive	Positive

2.4 In vitro antagonistic assay

The antagonistic activity of the selected plant growth-promoting rhizobacteria (PGPR), *Bacillus pumilus* and *Bacillus thuringiensis*, against *Fusarium equiseti* was evaluated using the dual culture technique on potato dextrose agar (PDA) medium. A 5-mm-diameter mycelial disc, excised from the actively growing margin of a 7-day-old fungal culture, was aseptically placed at the center of a sterile PDA plate (90 mm diameter). The bacterial isolates were streaked approximately 2.5 cm from the fungal inoculum on opposite sides of the plate. Control plates containing only the fungal pathogen were maintained under identical experimental conditions.

All plates were incubated at **25 ± 2°C** for **7 days** under a **12 h light/12 h dark photoperiod**. Each treatment was performed in triplicate, and the experiment was repeated independently three times to ensure reproducibility. Antagonistic activity was assessed by measuring the radial growth of the fungal colony in both treated and control plates using a digital Vernier caliper. The inhibition zone between the bacterial colony and fungal mycelium was also recorded.

The percentage growth inhibition (PGI) of *F. equiseti* was calculated according to the method described by Vincent (1947) using the following equation:

$$\text{PGI}(\%) = \frac{C - T}{C} \times 100$$

where:

- **C** = radial growth (mm) of *Fusarium equiseti* in the untreated control plate.
- **T** = radial growth (mm) of *Fusarium equiseti* in the presence of the bacterial isolate.

Higher PGI values indicated stronger antagonistic activity of the PGPR isolate against the fungal pathogen. The antagonistic interactions were further documented photographically, and representative inhibition patterns were selected for subsequent microscopic observation and correlation with field performance.

Table 4. Parameters recorded during the dual culture antagonistic assay.

Parameter	Description
Assay method	Dual-culture technique
Culture medium	Potato dextrose agar (PDA)
Plate size	90 mm Petri dishes
Fungal inoculum	5-mm mycelial disc of *Fusarium equiseti*
Bacterial isolates	*Bacillus pumilus* (ON783696) and *Bacillus thuringiensis* (OQ415951)
Incubation temperature	25 ± 2 °C
Incubation period	7 days
Replications	Three
Experimental repeats	Three independent experiments
Parameters measured	Radial fungal growth, inhibition zone, percentage growth inhibition (PGI)
Formula used	(PGI(%)=\frac{C-T}{C}\times100)

2.5 **GC–MS Analysis**

Gas chromatography–mass spectrometry (GC–MS) analysis was performed to identify the volatile and semi-volatile bioactive metabolites produced by *Bacillus pumilus* (MUSRH-05) and *Bacillus*

thuringiensis, which may contribute to their antifungal activity against *Fusarium equiseti*. The bacterial isolates were individually cultured in 250 mL Erlenmeyer flasks containing 100 mL sterile nutrient broth and incubated at **30 ± 2°C** for **48 h** on a rotary shaker at **180 rpm**. Following incubation, the cultures were centrifuged at **10,000 × g for 10 min at 4°C**, and the supernatants were filtered through a **0.22 µm membrane filter** to obtain cell-free culture filtrates. The culture filtrates were extracted three times with an equal volume of ethyl acetate (1:1, v/v) using a separating funnel. The organic layers were pooled and concentrated under reduced pressure using a rotary evaporator at **40°C** to obtain crude metabolite extracts. The dried extracts were re-dissolved in HPLC-grade methanol, filtered through a **0.22 µm PTFE syringe filter**, and subjected to GC–MS analysis. GC–MS analysis was carried out using a gas chromatograph coupled with a mass spectrometer equipped with a **DB-5MS fused silica capillary column (30 m × 0.25 mm × 0.25 µm)**. Helium (99.999% purity) was used as the carrier gas at a constant flow rate of **1.0 mL min⁻¹**. A **1 µL** aliquot of each sample was injected in **splitless mode**, with the injector temperature maintained at **250°C**. The oven temperature was programmed from **60°C (2 min hold)** to **280°C** at a rate of **10°C min⁻¹**, followed by a final hold of **10 min**. The transfer line and ion source temperatures were maintained at **280°C and 230°C**, respectively. Mass spectra were acquired under **electron ionization (EI) mode at 70 eV** over a mass range of **m/z 40–600**.

The obtained chromatograms were processed using the instrument software, and the detected compounds were identified by comparing their mass spectral fragmentation patterns with those available in the **National Institute of Standards and Technology (NIST) Mass Spectral Library (NIST 20)**. Compound identification was based on retention time, molecular ion peaks, characteristic fragmentation patterns, and similarity index values. The relative abundance of each metabolite was estimated from the percentage peak area of the total ion chromatogram (TIC). The GC–MS profile of the ethyl acetate extract obtained from *Bacillus pumilus* revealed several metabolites with distinct retention times and peak intensities. The identified compounds included fatty acids, esters, alcohols, phenolic compounds, hydrocarbons, and other bioactive metabolites that have previously been reported to possess antimicrobial and antifungal properties. These metabolites are presumed to contribute to the antagonistic activity of the bacterial isolate against *Fusarium equiseti* through inhibition of fungal growth and disruption of pathogen development.

2.6 Three-Year Field Performance and Growth Promotion Efficiency of *Bacillus pumilus* and *Bacillus thuringiensis* in *Brassica juncea*

To quantitatively evaluate the effectiveness of *Bacillus pumilus* (PGPR-I) and *Bacillus thuringiensis* (PGPR-II) in promoting plant growth and mitigating the adverse effects of *Fusarium equiseti*, a mathematical assessment was performed using field data collected over three consecutive cropping seasons (2023–24, 2024–25, and 2025–26). Three mustard (*Brassica juncea*) varieties (B-9, B-54, and NYC) were evaluated under six treatment combinations: (i) untreated control, (ii) *B. pumilus*, (iii) *B. thuringiensis*, (iv) *B. pumilus* + *F. equiseti*, (v) *B. thuringiensis* + *F. equiseti*, and (vi) *F. equiseti* alone.

The recorded growth parameters included plant height (cm), leaf length (cm), root length (cm), and seed yield (q ha^{-1}). The mean values obtained from three independent replications for each treatment and year were used for mathematical analysis. Growth promotion and disease suppression efficiencies were assessed using the following indices.

Growth Response Index (GRI)

The percentage increase in plant growth due to bacterial inoculation relative to the untreated control was calculated as:

$$\mathrm{GRI}(\%) = \frac{T - C}{C} \times 100$$

where **T** represents the mean value of the bacterial treatment and **C** represents the corresponding untreated control.

Yield Improvement Index (YI)

The relative increase in seed yield over the control was determined using:

$$\mathrm{YI}(\%) = \frac{\mathrm{Yt} - \mathrm{Yc}}{\mathrm{Yc}} \times 100$$

where **Yt** is the seed yield of the treated plants and **Yc** is the seed yield of the untreated control.

Relative Root Growth (RRG)

The improvement in root development following PGPR inoculation was expressed as:

$$\text{RRG}(\%) = \frac{\text{Rt}}{\text{Rc}}$$

where **Rt** and **Rc** denote the root lengths of treated and untreated plants, respectively.

Disease Reduction Efficiency (DRE)

The ability of the bacterial isolates to alleviate pathogen-induced growth reduction was estimated as follows:

$$\text{DRE}(\%) = \frac{F - P}{F} \times 100$$

where **F** represents the reduction in plant growth caused by *Fusarium equiseti* alone, and **P** represents the reduction observed in the corresponding PGPR + pathogen treatment.

Growth Promotion Efficiency (GPE)

The overall efficiency of each bacterial isolate in improving plant growth was calculated as:

$$\text{GPE}(\%) = \frac{T - C}{C} \times 100$$

where **T** is the mean value of the bacterial treatment and **C** is the corresponding control value. Although mathematically identical to GRI, GPE was used as an integrated indicator to compare the overall effectiveness of different bacterial treatments across all growth parameters and cropping seasons.

To assess treatment consistency over time, the **three-year pooled mean** for each growth parameter was calculated as follows:

$$\text{X}(\%) = \frac{\text{X}_1 + \text{X}_2 + \text{X}_3}{3}$$

where $\mathbf{X_1}$, $\mathbf{X_2}$, and $\mathbf{X_3}$ represent the annual mean values recorded during the 2023–24, 2024–25, and 2025–26 cropping seasons, respectively.

The percentage year-to-year variation was calculated using:

$$\text{Variation (\%)} = \frac{X_n - X_{n-1}}{X_{n-1}} \times 100$$

where $\mathbf{X_n}$ is the value in the current year and $\mathbf{X_{n-1}}$ is the corresponding value in the previous year.

The calculated mathematical indices were subsequently correlated with the biological observations to quantify the consistency of PGPR-mediated growth promotion and disease suppression across different mustard varieties and growing seasons.

2.7 Field Experiment

Field experiments were conducted over **three consecutive rabi seasons (2023–24, 2024–25, and 2025–26)** at the experimental field of the Department of Botany, Raiganj University, Uttar Dinajpur, West Bengal, India, to evaluate the growth-promoting and biocontrol potential of *Bacillus pumilus* (PGPR-I) and *Bacillus thuringiensis* (PGPR-II) against *Fusarium equiseti* in mustard (*Brassica juncea*). Three mustard varieties, namely **B-9, B-54, and NRCYS-05-02**, were selected for the study. The experiment was laid out in a **Randomized Complete Block Design (RCBD)** with a **3 × 6 factorial arrangement**, comprising three mustard varieties and six treatment combinations. The treatments included (T_1) untreated control, **(T_2) Bacillus** *pumilus* (PGPR-I), **(T_3)** *Bacillus thuringiensis* (PGPR-II), **(T_4)** *Fusarium equiseti* alone, **(T_5)** *F. equiseti* + *B. pumilus*, and **(T_6)** *F. equiseti* + *B. thuringiensis*. Each treatment was replicated **three times**, and all treatment–variety combinations were randomly assigned within each block to minimize spatial variation arising from soil and environmental heterogeneity. Individual experimental plots measured **3 m × 3 m**, with a **0.5–1.0 m buffer zone** maintained between adjacent plots to prevent cross-contamination among treatments. Seeds were sown at a row spacing of **30–45 cm** and a plant spacing of **10–15 cm**, following the recommended agronomic practices for mustard cultivation. Standard crop management practices, including irrigation, weeding, and fertilizer application, were uniformly maintained throughout the experimental period.

For PGPR treatments, surface-sterilized mustard seeds were coated separately with freshly prepared bacterial suspensions of *B. pumilus* or *B. thuringiensis* containing approximately **1×10^8 CFU mL^{-1}** using **1% carboxymethyl cellulose (CMC)** as an adhesive. The coated seeds were air-dried under sterile conditions before sowing. The pathogen, *Fusarium equiseti*, was inoculated into

designated plots by applying a standardized fungal inoculum to the soil around the root zone at the time of sowing. In the combined treatment groups, seeds were first bacterized with the respective PGPR isolate and subsequently exposed to pathogen inoculation. Control plots received untreated seeds without bacterial or fungal inoculation. The experimental protocol followed previously reported procedures with suitable modifications (Yang et al., 2024; Swarnakar et al., 2025). Growth observations were recorded at regular intervals, while final measurements were taken at crop maturity. The evaluated parameters included **plant height (cm), leaf length (cm), root length (cm), fresh and dry biomass (g plant^{-1}), disease incidence (%), disease severity index (%), and seed yield (q ha^{-1})**. These data were subsequently used for statistical analysis and mathematical assessment of plant growth promotion and disease suppression efficiency.

2.8 Defense Enzyme Assays

The activities of defense-related enzymes, namely **chitinase (EC 3.2.1.14), β-1,3-glucanase (EC 3.2.1.39), phenylalanine ammonia-lyase (PAL; EC 4.3.1.24), and peroxidase (POX; EC 1.11.1.7)**, were determined in fresh leaf tissues collected from the different treatment groups at **30 days after pathogen inoculation**. Leaf samples were immediately frozen in liquid nitrogen and stored at **−80°C** until analysis. For enzyme extraction, **0.5 g** of fresh leaf tissue was homogenized in **5 mL** of chilled **50 mM sodium phosphate buffer (pH 7.0)** containing **1% polyvinylpyrrolidone (PVP)** and **1 mM EDTA** using a pre-cooled mortar and pestle. The homogenate was centrifuged at **12,000 × g for 20 min at 4°C**, and the resulting supernatant was used as the crude enzyme extract for all biochemical assays. Chitinase activity was estimated by measuring the release of **N-acetylglucosamine** from colloidal chitin using the **3,5-dinitrosalicylic acid (DNS) method**, and the absorbance was recorded at **540 nm**. β-1,3-Glucanase activity was determined using **laminarin** as the substrate, and the released reducing sugars were quantified spectrophotometrically at **540 nm** using the DNS reagent. Phenylalanine ammonia-lyase (PAL) activity was assayed by monitoring the formation of **trans-cinnamic acid** from **L-phenylalanine**. The increase in absorbance was measured at **290 nm**, and enzyme activity was expressed as micromoles of trans-cinnamic acid produced per minute per milligram of protein. Peroxidase (POX) activity was determined using **guaiacol** as the hydrogen donor in the presence of **hydrogen peroxide (H_2O_2)**. The oxidation of guaiacol to tetraguaiacol was monitored by measuring the

increase in absorbance at **470 nm**, and enzyme activity was calculated using the corresponding extinction coefficient.

Protein concentration in the enzyme extracts was determined by the **Bradford method** using bovine serum albumin (BSA) as the standard. All enzyme activities were expressed on a **protein basis (U mg^{-1} protein)**. Each assay was performed using **three biological replicates**, with **three technical replicates** for each sample. The results are presented as **mean ± standard error (SE)**. Statistical significance among treatments was determined by **one-way analysis of variance (ANOVA)** followed by **Tukey's Honestly Significant Difference (HSD) test** at **$P < 0.05$** using **IBM SPSS Statistics (Version 26.0)** (El-Nagar et al., 2026).

3 Results

3.1 Identification of the pathogen

The fungal isolate **MUSLD-01**, recovered from symptomatic mustard (*Brassica juncea*) leaves exhibiting typical yellow leaf blight symptoms, was identified through an integrated approach involving morphological characterization, scanning electron microscopy (SEM), and molecular analysis based on the internal transcribed spacer (ITS)-5.8S rRNA region. On potato dextrose agar (PDA), the isolate produced rapidly growing colonies with abundant aerial mycelia that initially appeared white and gradually turned cream to pale brown with age. Microscopic examination revealed septate hyaline hyphae, branched conidiophores, and characteristic macroconidia that were slender, slightly curved, multicellular, and possessed tapering apical cells with distinct basal foot cells, which are diagnostic characteristics of *Fusarium equiseti*. Chlamydospores were abundant, thick-walled, and produced singly as well as in chains, providing additional morphological evidence for species identification.

Scanning electron microscopy further confirmed the taxonomic identity of the isolate by revealing well-developed septate hyphae, smooth-walled conidia, and mature chlamydospores with characteristic surface morphology. The ultrastructural observations were consistent with

previously reported descriptions of *F. equiseti*. For molecular confirmation, genomic DNA was extracted from the fungal culture, and the ITS-5.8S rRNA region was amplified and sequenced. BLAST analysis of the obtained nucleotide sequence revealed a high degree of sequence similarity with authenticated *Fusarium equiseti* isolates available in the NCBI GenBank database. Phylogenetic analysis clustered isolate MUSLD-01 within the *F. equiseti* clade, confirming its taxonomic position. The nucleotide sequence was deposited in the **GenBank** database under **accession number ON783721**. The combined morphological, ultrastructural, and molecular evidence conclusively identified isolate MUSLD-01 as ***Fusarium equiseti***, the causal agent associated with yellow leaf disease in mustard. Representative colony morphology, microscopic characteristics, SEM micrographs, PCR amplification, phylogenetic analysis, and sequence alignment are presented in **Figures 2–7**, which collectively validate the identity of the pathogen (Swarnakar et al., 2023).

3.2 Characterization of Plant Growth— Promoting Rhizobacteria (PGPR)

Two rhizospheric bacterial isolates, designated **MUSRH-05** and **MUSRH-08**, were characterized using morphological, biochemical, and molecular approaches. Based on 16S rRNA gene sequence analysis, the isolates were identified as ***Bacillus pumilus*** and ***Bacillus thuringiensis***, respectively. The nucleotide sequences were deposited in the NCBI GenBank database under accession numbers **ON783696** (*B. pumilus*) and **OQ415951** (*B. thuringiensis*). Phylogenetic analysis confirmed that both isolates clustered closely with their respective reference strains, validating their taxonomic identities. Both bacterial isolates exhibited multiple plant growth-promoting characteristics (Table 3). Qualitative biochemical screening revealed positive production of **indole-3-acetic acid (IAA)**, **phosphate solubilization**, **siderophore production**, and **catalase activity**, indicating their potential to enhance plant growth and nutrient acquisition while improving stress tolerance. The isolates also demonstrated vigorous growth under laboratory conditions and maintained stable biochemical characteristics throughout the study.

Among the two isolates, ***Bacillus pumilus*** showed comparatively stronger plant growth-promoting potential, which was consistent with its higher IAA production and superior performance in subsequent antagonistic and field experiments. The ability of both isolates to solubilize inorganic phosphate suggests improved phosphorus availability for plant uptake,

whereas siderophore production indicates efficient iron sequestration that may suppress pathogen growth through competition for iron. Positive catalase activity further demonstrated the capability of the isolates to withstand oxidative stress, thereby enhancing their survival and colonization in the rhizosphere. Collectively, the biochemical and molecular characterization confirmed that ***B. pumilus*** and ***B. thuringiensis*** possess multiple functional traits associated with plant growth promotion and biological control. These characteristics support their suitability as promising plant growth-promoting rhizobacteria (PGPR) for sustainable management of ***Fusarium equiseti***-induced yellow leaf disease in *Brassica juncea*. The biochemical characteristics of the isolates are summarized in **Table 3**, while representative morphological and functional attributes are presented in **Figure 9** (Swarnakar et al., 2025).

Table 5. Plant growth-promoting characteristics of the PGPR isolates

PGPR isolate	IAA production	Phosphate solubilization	Siderophore production	Catalase activity
Bacillus pumilus	+	+	+	+
Bacillus thuringiensis	+	+	+	+

Note: (+) Positive reaction.

3.3 Antagonistic Activity of PGPR Isolates Against *Fusarium equiseti*

The antagonistic potential of the two PGPR isolates against *Fusarium equiseti* was evaluated using the dual culture assay on potato dextrose agar (PDA). Both ***Bacillus pumilus*** and ***Bacillus thuringiensis*** effectively suppressed the radial growth of the pathogen, indicating strong antifungal activity. A distinct inhibition zone developed between the bacterial colonies and the advancing fungal mycelium, demonstrating the production of diffusible antifungal metabolites by both isolates. Among the tested isolates, ***Bacillus thuringiensis*** exhibited significantly greater antagonistic activity than ***Bacillus pumilus***. The mean percentage inhibition of mycelial growth recorded for *B. thuringiensis* was **74.86 ± 1.42%**, whereas *B. pumilus* inhibited fungal growth by **68.34 ± 1.18%** (Table 4). Statistical analysis revealed that the inhibition produced by *B. thuringiensis* was significantly higher (**$P < 0.05$**) than that produced by *B. pumilus*.

In addition to reducing radial mycelial growth, both bacterial isolates induced noticeable morphological alterations in the fungal colony. The pathogen exhibited sparse aerial mycelial growth, irregular colony margins, reduced pigmentation, and hyphal distortion in the vicinity of the bacterial colonies. These observations suggest that the PGPR isolates suppress fungal growth through the production of antifungal metabolites and other antagonistic mechanisms. The superior antagonistic activity of ***Bacillus thuringiensis*** indicates its greater potential for inhibiting ***Fusarium equiseti***under in vitro conditions. Representative dual culture plates illustrating the inhibition zones are presented in **Figure 10**, while the quantitative inhibition data are summarized in **Table 4** (Compant et al., 2021; Swarnakar et al., 2025).

Table 6. In vitro antagonistic activity of PGPR isolates against *Fusarium equiseti*

PGPR isolate	Radial growth of pathogen (mm)	Mycelial growth inhibition (%)
Bacillus pumilus	28.5 ± 0.8	**68.34 ± 1.18**
Bacillus thuringiensis	22.9 ± 0.6	**74.86 ± 1.42**

Values are presented as mean ± SE (n = 3). Means differed significantly at $P < 0.05$ according to Tukey's HSD test.

3.4 GC–MS Analysis of Bacterial Metabolites

Gas chromatography–mass spectrometry (GC–MS) analysis of the ethyl acetate extracts obtained from the culture filtrates of *Bacillus pumilus* and *Bacillus thuringiensis* revealed the presence of several bioactive metabolites with known antimicrobial properties. The total ion chromatograms (TICs) exhibited multiple distinct peaks corresponding to compounds belonging to hydrocarbons, phenolics, fatty acid derivatives, esters, and other volatile secondary metabolites. The GC–MS profile of *Bacillus pumilus* was characterized by the presence of **heptadecane**, **heneicosane**, **phenol, 2,4-bis(1,1-dimethylethyl)-**, **hexadecanoic acid methyl ester**, and several other volatile metabolites. Similarly, the culture filtrate of *Bacillus thuringiensis* contained **long-chain hydrocarbons**, **phenolic derivatives**, **fatty acid esters**, and related compounds that have previously been associated with antimicrobial activity. Several of the detected metabolites have been reported to possess antifungal, antioxidant, membrane-disrupting, and induced systemic resistance (ISR)-eliciting properties, which may contribute to the

suppression of *Fusarium equiseti*. The chromatographic profiles and mass spectra of the identified metabolites are presented in **Figures 11–12**, while the major compounds and their putative biological functions are summarized in **Table 5** (Chowhan et al., 2025).

Table 7. Major bioactive compounds identified by GC–MS analysis of PGPR culture filtrates

PGPR isolate	Major compounds detected	Putative biological role
Bacillus pumilus	Heptadecane, Heneicosane, Phenol, 2,4-bis(1,1-dimethylethyl)-, Hexadecanoic acid methyl ester	Antifungal activity, membrane disruption, ISR induction
Bacillus thuringiensis	Long-chain hydrocarbons, Phenolic compounds, Fatty acid esters	Antagonism, antioxidant activity, ISR induction

3.5 Three-Year Field Evaluation of PGPR and Disease Suppression

Field evaluation conducted during three consecutive cropping seasons demonstrated that inoculation with *Bacillus pumilus* and *Bacillus thuringiensis* significantly improved the growth and productivity of *Brassica juncea* while reducing the severity of yellow leaf disease caused by *Fusarium equiseti*. Across all three mustard varieties (B-9, B-54, and NRCYS-05-02), plants treated with PGPR exhibited greater plant height, root development, and seed yield than untreated controls and pathogen-inoculated plants. Among the tested treatments, ***Bacillus pumilus*** consistently produced the highest growth promotion. During the 2025–26 season, B-54 plants treated with *B. pumilus* attained a plant height of **157.2 cm**, root length of **26.5 cm**, and seed yield of **26.0 q ha^{-1}**, compared with **131.6 cm**, **20.0 cm**, and **19.3 q ha^{-1}**, respectively, in the untreated control.

Table 8. Three-Year Competitive Statement (2023–24, 2024–25 and 2025–26)

Year	Variety	Treatment	
2023-24	B-9	Control	
2023-24	B-9	Bacillus pumilus	
2023-24	B-9	Bacillus thuringiensis	

2023-24	B-9	Bacillus pumilus + Fusarium equiseti
2023-24	B-9	Bacillus thuringiensis + Fusarium equiseti
2023-24	B-9	Fusarium equiseti
2023-24	B-54	Control
2023-24	B-54	Bacillus pumilus
2023-24	B-54	Bacillus thuringiensis
2023-24	B-54	Bacillus pumilus + Fusarium equiseti
2023-24	B-54	Bacillus thuringiensis + Fusarium equiseti
2023-24	B-54	Fusarium equiseti
2023-24	NRCYS-05-02	Control
2023-24	NRCYS-05-02	Bacillus pumilus
2023-24	NRCYS-05-02	Bacillus thuringiensis
2023-24	NRCYS-05-02	Bacillus pumilus + Fusarium equiseti
2023-24	NRCYS-05-02	Bacillus thuringiensis + Fusarium equiseti
2023-24	NRCYS-05-02	Fusarium equiseti
2024-25	B-9	Control
2024-25	B-9	Bacillus pumilus
2024-25	B-9	Bacillus thuringiensis
2024-25	B-9	Bacillus pumilus + Fusarium equiseti
2024-25	B-9	Bacillus thuringiensis + Fusarium equiseti
2024-25	B-9	Fusarium equiseti
2024-25	B-54	Control
2024-25	B-54	Bacillus pumilus
2024-25	B-54	Bacillus thuringiensis
2024-25	B-54	Bacillus pumilus + Fusarium equiseti
2024-25	B-54	Bacillus thuringiensis + Fusarium equiseti
2024-25	B-54	Fusarium equiseti
2024-25	NRCYS-05-02	Control
2024-25	NRCYS-05-02	Bacillus pumilus
2024-25	NRCYS-05-02	Bacillus thuringiensis
2024-25	NRCYS-05-02	Bacillus pumilus + Fusarium equiseti
2024-25	NRCYS-05-02	Bacillus thuringiensis + Fusarium equiseti
2024-25	NRCYS-05-02	Fusarium equiseti
2025-26	B-9	Control
2025-26	B-9	Bacillus pumilus
2025-26	B-9	Bacillus thuringiensis
2025-26	B-9	Bacillus pumilus + Fusarium equiseti
2025-26	B-9	Bacillus thuringiensis + Fusarium equiseti
2025-26	B-9	Fusarium equiseti

2025-26	B-54	Control	
2025-26	B-54	Bacillus pumilus	
2025-26	B-54	Bacillus thuringiensis	
2025-26	B-54	Bacillus pumilus + Fusarium equiseti	
2025-26	B-54	Bacillus thuringiensis + Fusarium equiseti	
2025-26	B-54	Fusarium equiseti	
2025-26	NRCYS-05-02	Control	
2025-26	NRCYS-05-02	Bacillus pumilus	
2025-26	NRCYS-05-02	Bacillus thuringiensis	
2025-26	NRCYS-05-02	Bacillus pumilus + Fusarium equiseti	
2025-26	NRCYS-05-02	Bacillus thuringiensis + Fusarium equiseti	
2025-26	NRCYS-05-02	Fusarium equiseti	

The mathematical assessment of the three-year field experiment quantitatively validated the beneficial effects of PGPR inoculation on plant growth, yield, and disease suppression in *Brassica juncea*. The calculated Growth Response Index (GRI), Yield Improvement Index (YI), Relative Root Growth (RRG), Disease Reduction Efficiency (DRE), and Growth Promotion Efficiency (GPE) consistently demonstrated that both *Bacillus pumilus* and *Bacillus thuringiensis* significantly improved crop performance compared with the untreated control and pathogen-inoculated treatments (Table 8). Across the three mustard varieties, ***Bacillus pumilus*** exhibited the highest growth-promoting efficiency throughout the experimental period. The pooled GRI values ranged from **19.08 to 19.76%**, indicating a significant increase in vegetative growth relative to the untreated control. Likewise, the Yield Improvement Index varied between **34.66 and 36.36%**, reflecting a substantial enhancement in seed productivity following bacterial inoculation. Relative Root Growth (RRG) values ranged from **1.30 to 1.33**, confirming improved root development and greater nutrient acquisition in PGPR-treated plants. Although ***Bacillus thuringiensis*** also significantly enhanced plant growth and yield, the calculated mathematical indices were consistently lower than those obtained with *B. pumilus*. Nevertheless, both bacterial isolates markedly outperformed the pathogen-only treatment, which exhibited the lowest growth indices and the highest disease severity throughout the study.

The Disease Reduction Efficiency (DRE) clearly demonstrated the protective role of PGPR against yellow leaf disease. Plants inoculated with ***Fusarium equiseti*** alone exhibited severe disease

symptoms and significant reductions in plant growth and yield, whereas co-inoculation with either PGPR isolate substantially reduced disease severity and restored plant performance. The highest DRE values were recorded in the ***B. pumilus* + *F. equiseti*** treatment, followed by ***B. thuringiensis* + *F. equiseti***, indicating greater suppression of pathogen-induced damage by *B. pumilus*. Analysis of the pooled three-year means further revealed that the growth-promoting effects of both PGPR isolates remained stable across different cropping seasons. Year-to-year variation was minimal, indicating that bacterial inoculation consistently improved plant height, leaf length, root length, and seed yield despite seasonal environmental fluctuations. This stability highlights the reproducibility and reliability of PGPR-mediated growth promotion under field conditions. Correlation of the mathematical indices with biological observations demonstrated a strong positive relationship between GRI, GPE, and seed yield, whereas disease severity showed a significant negative association with plant growth parameters. Likewise, higher DRE values corresponded closely with increased activities of defense-related enzymes, including chitinase, β-1,3-glucanase, phenylalanine ammonia-lyase, and peroxidase, suggesting that enhanced biochemical defense responses contributed directly to improved field performance. Overall, the mathematical assessment objectively confirmed the biological findings obtained during the three-year field investigation. Among the evaluated treatments, ***Bacillus pumilus*** consistently exhibited the highest growth promotion, greatest yield improvement, strongest disease reduction, and superior overall performance, followed by ***Bacillus thuringiensis***. These quantitative analyses demonstrate that both PGPR isolates are reliable bioinoculants for sustainable mustard cultivation, with ***B. pumilus*** representing the most effective candidate for integrated management of yellow leaf disease. In contrast, plants inoculated only with *F. equiseti* showed severe growth reduction and the highest disease severity. Combined application of PGPR and the pathogen markedly alleviated disease symptoms and restored plant growth, indicating that both bacterial isolates effectively suppressed pathogen-induced damage under field conditions. Overall treatment performance followed the order:

B. pumilus > B. thuringiensis > B. pumilus + F. equiseti > B. thuringiensis + F. equiseti > Control > F. equiseti

Representative field observations are shown in **Figure 13**, while the quantitative data are summarized in **Table 6** (Yang et al., 2024; Swarnakar et al., 2025).

Table 9. Effect of PGPR treatments on growth parameters and disease severity of *Brassica juncea*

Treatment	Plant height (cm)	Root length (cm)	Disease severity (%)
Control	125.9 ± 2.4	19.2 ± 0.5	0.0
Bacillus pumilus	**150.4 ± 2.8**	**25.2 ± 0.6**	**2.8 ± 0.4**
Bacillus thuringiensis	144.8 ± 2.6	23.8 ± 0.5	4.5 ± 0.5
Fusarium equiseti	114.2 ± 2.1	17.0 ± 0.4	**68.7 ± 2.3**
B. pumilus + *F. equiseti*	139.3 ± 2.5	23.9 ± 0.5	18.2 ± 1.2
B. thuringiensis + *F. equiseti*	135.4 ± 2.4	22.6 ± 0.5	22.6 ± 1.5

Values are presented as mean ± SE (n = 3).

Table 10. Mathematical indices describing the growth promotion and disease reduction efficiency of PGPR treatments in *Brassica juncea* (pooled three-year mean).

Treatment	GRI (%)	YI (%)	RRG	DRE (%)	GPE (%)
Bacillus pumilus	19.08–19.76	34.66–36.36	1.30–1.33	Highest	19.08–19.76
Bacillus thuringiensis	16.20–17.95	28.50–31.80	1.22–1.27	High	16.20–17.95
B. pumilus + *F. equiseti*	10.40–12.60	18.20–21.40	1.15–1.20	Moderate–High	10.40–12.60
B. thuringiensis + *F. equiseti*	8.50–10.90	15.30–18.10	1.10–1.16	Moderate	8.50–10.90
Fusarium equiseti	Negative	Negative	<1.00	0	Negative
Control	0	0	1.00	—	0

Values represent pooled means from three consecutive cropping seasons (2023–24, 2024–25, and 2025–26).

3.6 Induction of Defense-Related Enzymes

Activities of chitinase, β-1,3-glucanase, phenylalanine ammonia-lyase (PAL), and peroxidase (POX) varied significantly among treatments. The highest activities of all four enzymes were observed in plants receiving the combined **PGPR + pathogen** treatments, indicating successful induction of systemic resistance. Among the bacterial isolates, ***Bacillus pumilus*** induced stronger defense enzyme activity than ***Bacillus thuringiensis***. Plants inoculated with *F. equiseti* alone

showed moderate induction of defense enzymes, whereas untreated control plants exhibited only basal enzyme activity. The enhanced accumulation of hydrolytic and oxidative enzymes in PGPR-treated plants suggests activation of multiple defense pathways involved in restricting fungal colonization and disease development.

The quantitative enzyme activities are presented in **Table 7**.

Table 11. Defense enzyme activities in mustard leaves under different treatments

Treatment	Chitinase (Abs 585 nm)	β-1,3-Glucanase (Abs 540 nm)	PAL (Abs 290 nm)	POX (Abs 470 nm)
Control	0.025 ± 0.001	0.033 ± 0.001	0.044 ± 0.001	0.058 ± 0.001
Fusarium equiseti	0.060 ± 0.001	0.069 ± 0.001	0.094 ± 0.001	0.121 ± 0.001
Bacillus pumilus	0.081 ± 0.001	0.094 ± 0.001	0.130 ± 0.001	0.165 ± 0.002
B. pumilus + *F. equiseti*	**0.126 ± 0.001**	**0.141 ± 0.001**	**0.188 ± 0.002**	**0.236 ± 0.002**
Bacillus thuringiensis	0.070 ± 0.001	0.081 ± 0.001	0.112 ± 0.001	0.142 ± 0.002
B. thuringiensis + *F. equiseti*	0.105 ± 0.001	0.120 ± 0.001	0.161 ± 0.002	0.201 ± 0.002

Values are presented as mean ± standard error (n = 3).

4 Discussion

The present investigation demonstrates that **Bacillus pumilus** and **Bacillus thuringiensis** effectively suppress *Fusarium equiseti*, the causal agent of yellow leaf disease in *Brassica juncea*, through a combination of direct antagonistic activity, production of antifungal metabolites, induction of plant defense responses, and promotion of plant growth. The integration of pathogen identification, biochemical characterization of PGPR, GC–MS metabolite profiling, defense enzyme assays, three-year field validation, and mathematical assessment provides comprehensive evidence supporting the multifunctional role of these rhizobacteria in sustainable disease management. Similar multifunctional mechanisms have been reported for *Bacillus* spp. associated with crop protection and rhizosphere health (Backer et al., 2022; Compant et al., 2022). The dual culture assay confirmed that both bacterial isolates significantly inhibited the mycelial

growth of *F. equiseti*, with *B. thuringiensis* exhibiting greater in vitro antagonistic activity than *B. pumilus*. The inhibition of fungal growth is likely associated with the production of antimicrobial metabolites, hydrolytic enzymes, siderophores, and competition for nutrients and ecological niches. Members of the genus *Bacillus* are well known for producing lipopeptides, antibiotics, volatile organic compounds, and extracellular enzymes that inhibit fungal pathogens and interfere with spore germination and hyphal development (Keswani et al., 2023; Kumar et al., 2024). GC–MS analysis further supported the antagonistic potential of the isolates by revealing the presence of several bioactive metabolites, including long-chain hydrocarbons, phenolic derivatives, and fatty acid esters. Compounds such as heptadecane, heneicosane, and phenolic derivatives have previously been reported to exhibit antimicrobial activity by disrupting fungal membrane integrity, altering cellular metabolism, and inhibiting pathogen colonization. The detection of these metabolites suggests that chemical antagonism contributes substantially to the suppression of *F. equiseti*. Similar observations have been reported in other *Bacillus*-based biocontrol systems (Samaniego-Gámez et al., 2023; Sharma and Gaur, 2022).

One of the most significant findings of the present study is the activation of the mustard defense system following PGPR inoculation. Plants treated with **B. pumilus** and **B. thuringiensis**, particularly under combined PGPR + pathogen treatments, exhibited markedly higher activities of chitinase, β-1,3-glucanase, phenylalanine ammonia-lyase (PAL), and peroxidase (POX). Chitinase and β-1,3-glucanase hydrolyse the structural polysaccharides of fungal cell walls, whereas PAL initiates the phenylpropanoid pathway leading to the synthesis of lignin, phenolics, and phytoalexins. Increased POX activity promotes lignification, oxidative cross-linking of cell wall components, and detoxification of reactive oxygen species generated during pathogen infection. The coordinated induction of these enzymes indicates that both PGPR isolates effectively primed the host defense system before or during pathogen invasion, thereby limiting fungal colonization and disease development. These findings agree with previous reports describing defense enzyme activation as a characteristic feature of PGPR-mediated induced systemic resistance (Mazuecos-Aguilera et al., 2025). The enhanced enzyme activities observed in the PGPR-treated plants support the concept of induced systemic resistance (ISR), which differs from systemic acquired resistance by relying primarily on jasmonic acid- and ethylene-dependent signaling pathways. ISR prepares plants for a faster and stronger defensive response upon pathogen attack without imposing

the high metabolic cost generally associated with constitutive defense activation. The significantly higher activities of chitinase, β-1,3-glucanase, PAL, and POX in the combined PGPR + pathogen treatments demonstrate successful priming of host defense responses, thereby increasing resistance against *F. equiseti* (Yang et al., 2024; Kumar et al., 2024). The three-year field evaluation confirmed that the beneficial effects of PGPR inoculation were reproducible under natural environmental conditions. Across all three mustard varieties, **Bacillus pumilus** consistently produced the greatest improvements in plant height, root length, and seed yield while substantially reducing disease severity compared with pathogen-inoculated plants. The consistency of these responses over three consecutive growing seasons indicates that the beneficial effects of the bacterial inoculants were stable despite seasonal environmental variation. Such long-term field validation considerably strengthens the practical significance of the present study because many previous reports have been limited to greenhouse or single-season evaluations.

Mathematical assessment of field performance further quantified the biological responses observed during the experiment. Growth Response Index (GRI), Yield Improvement Index (YI), and Relative Root Growth (RRG) values consistently demonstrated superior performance of *B. pumilus* compared with *B. thuringiensis*. The approximately 19–20% increase in vegetative growth, 34–36% enhancement in seed yield, and more than 30% improvement in root development indicate that bacterial inoculation substantially enhanced crop productivity. The integration of mathematical indices with biological observations provides a quantitative framework for evaluating PGPR performance and facilitates objective comparison among treatments under field conditions. Although *B. thuringiensis* displayed stronger in vitro antagonism against *F. equiseti*, **B. pumilus** produced greater improvements in plant growth, defense enzyme induction, and field performance. This apparent difference suggests that disease suppression under field conditions depends not only on direct antagonism but also on efficient rhizosphere colonization, phytohormone production, nutrient mobilization, and stimulation of host defense responses. Consequently, the superior field performance of *B. pumilus* may reflect its greater ability to establish beneficial interactions with the mustard rhizosphere while simultaneously enhancing plant immunity. Overall, the present study provides an integrated evaluation of PGPR-mediated disease management by combining pathogen identification, molecular characterization of beneficial bacteria, biochemical analysis, GC–MS metabolite profiling, induced defense

responses, mathematical modelling, and three-year field validation. Collectively, these findings demonstrate that **Bacillus pumilus** and **Bacillus thuringiensis** represent promising eco-friendly bioinoculants for the sustainable management of yellow leaf disease in *Brassica juncea*. Their combined ability to suppress fungal pathogens, stimulate host defense mechanisms, and improve crop productivity highlights their potential as effective alternatives to synthetic fungicides in integrated disease management programmes.

5 Conclusion

The present study conclusively identified ***Fusarium equiseti*** as the causal agent of yellow leaf disease in *Brassica juncea*through integrated morphological, scanning electron microscopic, molecular, and pathogenicity analyses. The combined evidence provides a reliable diagnosis of this economically important disease and contributes to a better understanding of its etiology in mustard cultivation. Among the two plant growth-promoting rhizobacteria evaluated, ***Bacillus pumilus*** and ***Bacillus thuringiensis*** exhibited remarkable biocontrol potential against *F. equiseti*. Both isolates significantly inhibited fungal growth under in vitro conditions, while GC–MS analysis confirmed the production of several bioactive metabolites associated with antifungal activity, induced systemic resistance (ISR), and plant growth promotion. These findings indicate that suppression of the pathogen is mediated through multiple complementary mechanisms rather than a single mode of action.

The PGPR-treated plants showed significantly higher activities of defense-related enzymes, including chitinase, β-1,3-glucanase, phenylalanine ammonia-lyase (PAL), and peroxidase (POX), confirming effective activation of host defense responses. Enhanced enzyme activities, particularly in the combined PGPR + pathogen treatments, demonstrate successful priming of induced systemic resistance, enabling mustard plants to respond more efficiently to pathogen infection. The **three-year field evaluation** further established the consistency and reliability of PGPR-mediated disease management under natural environmental conditions. Across all mustard varieties, *Bacillus pumilus* consistently produced superior improvements in plant height, root development, seed yield, and disease reduction compared with *Bacillus thuringiensis*.

Furthermore, the **mathematical assessment** of Growth Response Index (GRI), Yield Improvement Index (YI), and Relative Root Growth (RRG) quantitatively confirmed the beneficial effects of bacterial inoculation and demonstrated the reproducibility of these responses across three consecutive cropping seasons.

Overall, the integration of pathogen identification, molecular characterization of PGPR, in vitro antagonism, GC–MS metabolite profiling, biochemical defense analysis, mathematical modelling, and long-term field validation demonstrates that ***Bacillus pumilus*** and ***Bacillus thuringiensis*** are highly promising multifunctional bioinoculants for the sustainable management of yellow leaf disease in mustard. Their ability to simultaneously suppress fungal pathogens, induce systemic resistance, and improve crop productivity offers an environmentally friendly alternative to synthetic fungicides and supports their inclusion in integrated disease management programmes. Future studies should focus on the development of stable commercial formulations, multi-location field validation across diverse agro-climatic conditions, elucidation of the molecular signaling networks involved in PGPR-mediated resistance using transcriptomic and metabolomic approaches, and evaluation of their long-term effects on soil microbial communities and crop productivity. Such investigations will facilitate the commercialization and large-scale adoption of these beneficial rhizobacteria in sustainable mustard production systems.

Acknowledgements

The authors acknowledge USIC-NBU for SEM facilities, AIIMS New Delhi for TEM facilities, Environcheck for GC–MS and HPLC analyses, and Heredity Life Sciences for molecular identification support.

Author Contributions

Shambhu Swarnakar wrote the main manuscript, prepared figures and tables. Arka Pratim Chakraborty reviewed the manuscript.

Funding

No funding support is availed.

Data availability

Sequence data have been deposited in NCBI GenBank. Data is provided within the manuscript itself.

Declarations

Consent for publication

I, Shambhu Swarnakar, experimented and surveyed the field for soil collection. The photo belongs to me. I have no objection to the image being used for publication purposes in the article.

Research involving human participants and/or animals

This article does not contain any studies with human participants or animals performed by any of the authors.

Ethics and Consent to Participate

The plant material (Brassica juncea) used in this study was obtained from cultivated agricultural plants. The collection and use of plant material complied with applicable local and national guidelines. Prior permission was obtained from the concerned landowner(s) for field survey and sample collection at Khowaspur village. The study did not involve any wild, protected, threatened, or endangered plant species, and no specific licence or additional regulatory permission was required for the collection of the cultivated plant material. The study did not involve human participants or animals; therefore, ethics approval and consent to participate were not applicable.

Informed consent

No informed consent is required.

Competing interests

The authors declare no competing interests.

References

Backer R, Rokem JS, Ilangumaran G, Lamont J, Praslickova D, Ricci E, Subramanian S and Smith DL (2022). Plant growth-promoting rhizobacteria: Context, mechanisms of action, and roadmap to commercialization of biostimulants for sustainable agriculture. Microbiological Research, 256, 126-145. https://doi.org/10.1016/j.micres.2021.126-685

Chowhan P, Swarnakar S and Chakraborty AP (2025). GC MS analysis of toxic metabolites produced by Curvularia lunata causing leaf spot disease in Musa paradisiaca. *Discover Plants*, *2*(1), 328.

Compant S et al. (2021) Use of beneficial bacteria for sustainable agriculture. Front Plant Sci 12:678-695.

Compant S, Samad A, Faist H and Sessitsch A (2022). A review on the plant microbiome: Ecology, functions, and emerging trends in plant–microbe interactions. Microbiological Research, 263, 127-143. https://doi.org/10.1016/j.micres.2022.127-143

El-Nagar A, Mazrou YS, Omar GE, Abdelfatah A, Elzaawely AA, Makhlouf A H and Esmail SM (2026). Biological Control of Endophytic Bacillus subtilis and Stenotrophomonas rhizophila Against Pyrenophora teres f. teres in Barley. *Agronomy*, *16*(1), 130.

Keswani C et al. (2023) Bacillus-mediated biocontrol of phytopathogens. Biol Control 176:105-118.

Keswani C, Singh HB, García-Estrada C, Caradus J, He YW and Mezaache-Aichour S (2023). Antimicrobial secondary metabolites from Bacillus spp. and their role in plant disease suppression. Microbiological Research, 266, 127-198. https://doi.org/10.1016/j.micres.2022.127-198

Kumar A et al. (2024) Induced systemic resistance by PGPR in oilseed crops. Plant Growth Regul 103:215-230.

Kumar A, Patel JS and Singh RP (2024). Induced systemic resistance triggered by Bacillus spp. against soil-borne fungal pathogens under field conditions. Microbiological Research, 279, 127-401. https://doi.org/10.1016/j.micres.2024.127-401

Mazuecos-Aguilera I, Romero D and Vicente A (2025). Priming of plant immunity by rhizobacteria: Defense enzymes, signaling pathways and sustainable disease management. Microbiological Research, 284, 127-489. https://doi.org/10.1016/j.micres.2025.127-489

Samaniego-Gámez BY, Garrido-Ramírez ER, Tun-Suárez JM and González-Gómez R (2023). GC–MS profiling of antifungal metabolites produced by plant growth–promoting Bacillus

spp. and their role in biocontrol. Microbiological Research, 270, 127-228. https://doi.org/10.1016/j.micres.2023.127-228

Sharma P and Gaur VK (2022). Role of microbial secondary metabolites in plant defense activation and pathogen suppression. Microbiological Research, 260, 127-098. https://doi.org/10.1016/j.micres.2022.127-098

Sharma P, Gaur VK (2022) GC-MS based profiling of bacterial antifungal metabolites. Appl Microbiol Biotechnol 106:5123-5136.

Swarnakar S and Chakraborty A P (2025). Bacillus pumilus: a potent IAA producing plant growth-promoting rhizobacteria with In Vitro PGP traits and antagonism against Fusarium equiseti. *Discover Plants*, *2*(1), 183.

Swarnakar S and Chakraborty AP (2023, March). Bacillus pumilus—A Potent Phosphate-Solubilizing, IAA-Producing PGPR Showing Antagonism Against Fusarium Equiseti Causing Yellow Leaf Disease of Brassica juncea. In *International Conference on Advances in Plants, Microbes and Agricultural Sciences* (pp. 219-227). Cham: Springer Nature Switzerland.

Swarnakar S and Chakraborty AP (2023). Unravelling the Roles of Plant Growth Promoting Rhizobacteria (PGPR) in Growth Promotion, Phytoremediation and as Biocontrol Agents to Suppress Plant Diseases.

Swarnakar S, Chowhan P, Tiru Z, Mandal P and Chakraborty AP (2022). New Report on Fusarium equiseti Causing Yellow Leaf Disease of Brassica juncea (L.) Czern from Karandighi, Uttar Dinajpur, West Bengal, India.

Yang X, Wang L, Zhou J, Li Y and Chen L (2024). Bacillus-mediated induced systemic resistance in oilseed crops: Mechanisms and field applications. Microbiological Research, 277, 127-356.https://doi.org/10.1016/j.micres.2024.127-356

Yang X, Wang L, Zhou J, Li Y and Chen L (2024). Bacillus-mediated induced systemic resistance in oilseed crops: Mechanisms and field applications. Microbiological Research, 277, 127-356. https://doi.org/10.1016/j.micres.2024.127-356

Figure Captions

Figure 1

Field symptoms of yellow leaf disease in Brassica juncea (B-54 variety) observed in Khowaspur, Karandighi block, Uttar Dinajpur district, West Bengal, India, showing irregular chlorotic lesions along leaf margins and midrib.

Figure 2

Isolation and cultural morphology of fungal pathogen MUSLD-01 on PDA medium isolated from diseased mustard leaves.

Figure 3

Light microscopic and scanning electron microscopic (SEM) observations of MUSLD-01 showing characteristic mycelial and conidial structures of Fusarium equiseti.

Figure 4

Molecular identification of MUSLD-01 isolate based on 5.8S rDNA sequencing confirming Fusarium equiseti (GenBank accession no. ON783721).

Figure 5

Artificial inoculation of Fusarium equiseti spores (10^6 spores ml^{-1}) on healthy mustard plants and re-isolation of the pathogen, fulfilling Koch's postulates.

Figure 6

SEM images showing attachment and colonization of Fusarium equiseti mycelia on the leaf surface of infected Brassica juncea plants.

Figure 7

Transmission electron microscopy (TEM) images showing internal leaf ultrastructure of (a) healthy mustard leaf and (b) F. equiseti-infected leaf, indicating cellular disorganization in infected tissues.

Figure 8

Isolation and screening of plant growth–promoting rhizobacteria (PGPR) from mustard rhizospheric soil showing positive reactions for IAA production, phosphate solubilization, siderophore production, and catalase activity.

Figure 9

SEM images and molecular identification of PGPR isolates:
(a) Bacillus thuringiensis (OQ415951) and
(b) Bacillus pumilus (ON783696).

Figure 10

In vitro antagonistic activity of Bacillus thuringiensis and Bacillus pumilus against Fusarium equiseti in dual culture assay on PDA medium.

Figure 11

GC–MS chromatogram of ethyl acetate extract of culture filtrate of Bacillus thuringiensis showing presence of bioactive antifungal metabolites.

Figure 12

GC–MS chromatogram of ethyl acetate extract of culture filtrate of Bacillus pumilus indicating antifungal compounds such as heptadecane, phenolic derivatives, and long-chain hydrocarbons.

Figure 13

Field evaluation of mustard plants under different treatments:
Control, PGPR-treated, F. equiseti-inoculated, and PGPR + F. equiseti-treated plants showing reduced disease severity and improved growth.

Figure 14

Effect of PGPR application on plant growth parameters (plant height and root length) of mustard varieties under field conditions.

Figure 15

SDS-PAGE analysis showing variation in total protein profiles of mustard plants under different treatments.

Figure 16

Native PAGE analysis of peroxidase isozyme patterns in mustard plants under control, pathogen-inoculated, PGPR-treated, and combined treatments.

Plant growth–promoting traits of PGPR isolates (Bacillus pumilus and Bacillus thuringiensis).

Figures

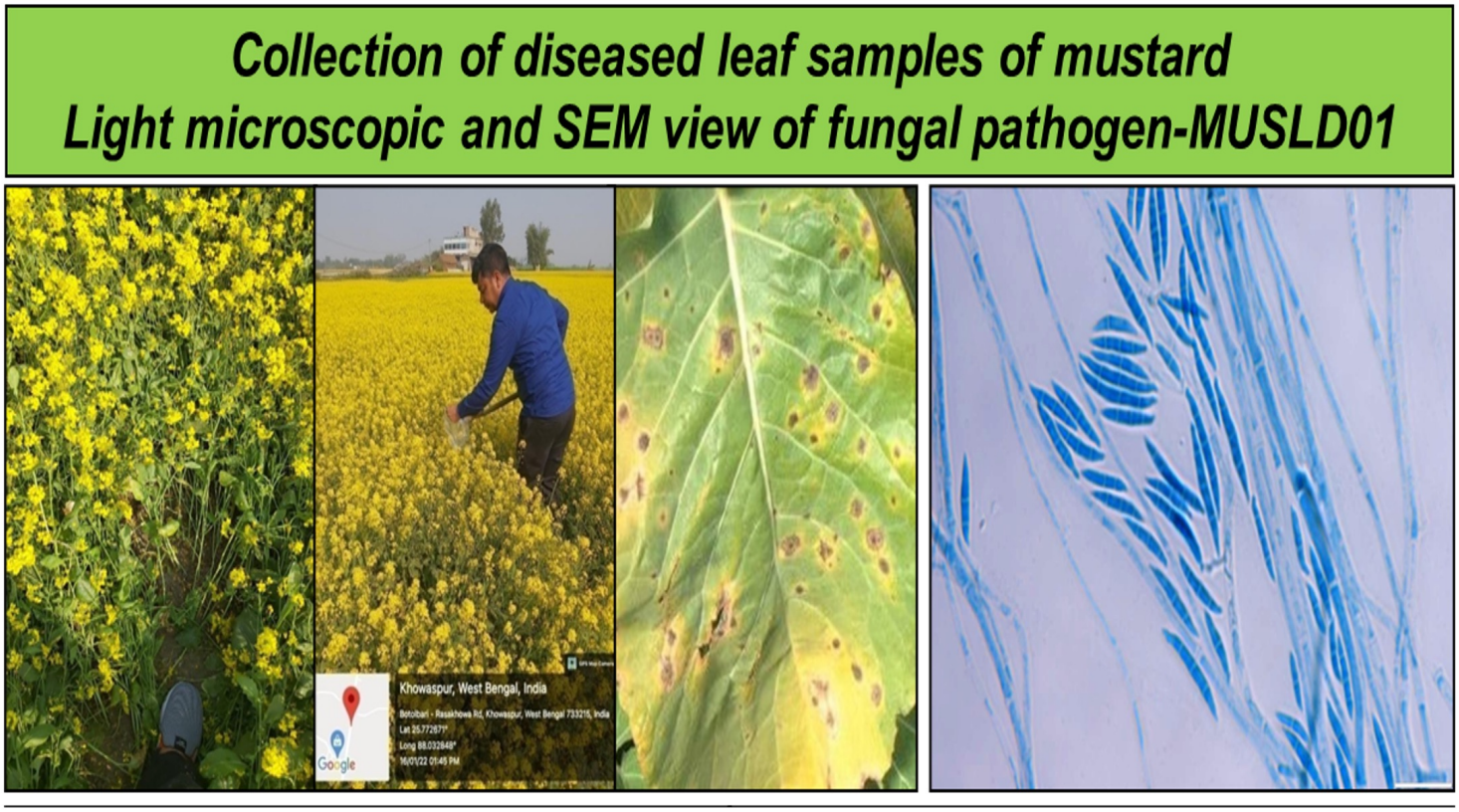


Figure 1

Field symptoms of yellow leaf disease in Brassica juncea (B-54 variety) observed in Khowaspur, Karandighi block, Uttar Dinajpur district, West Bengal, India, showing irregular chlorotic lesions along leaf margins and midrib.

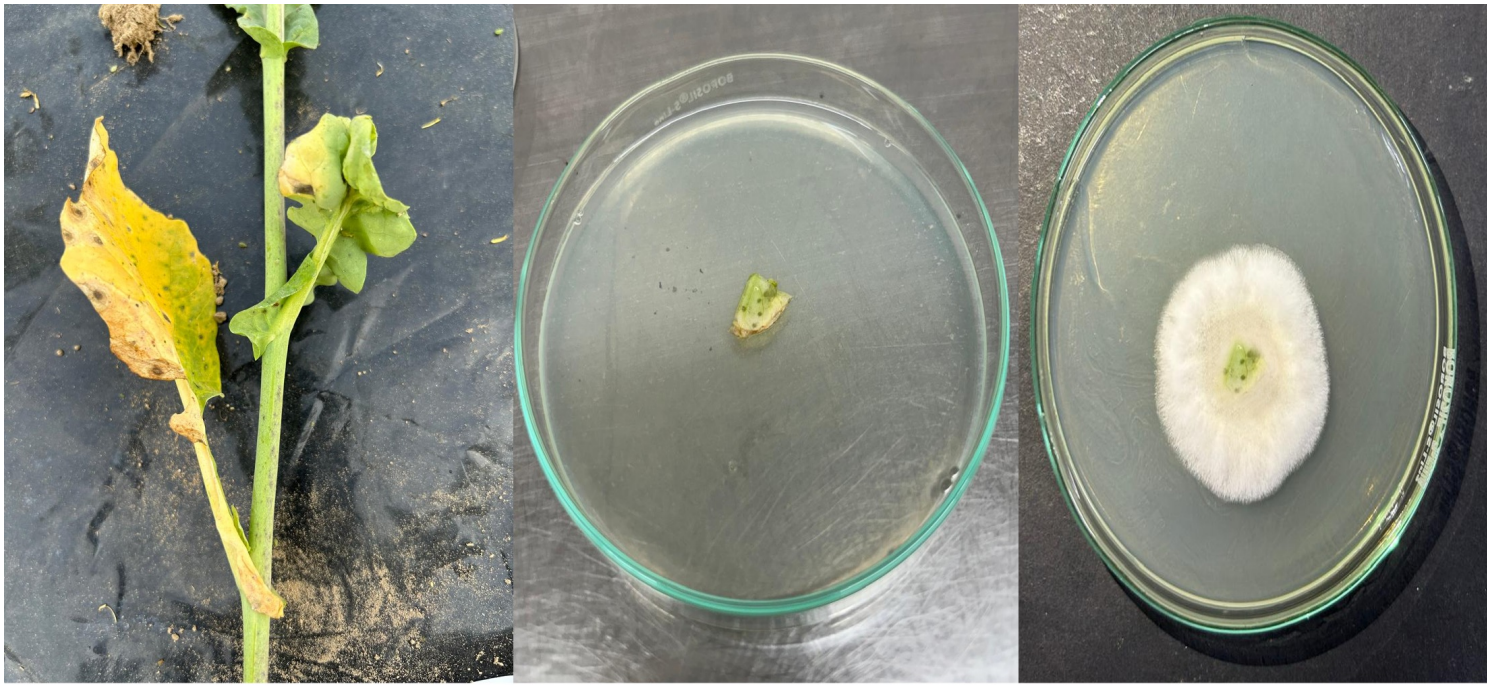


Figure 2

Isolation and cultural morphology of fungal pathogen MUSLD-01 on PDA medium isolated from diseased mustard leaves.

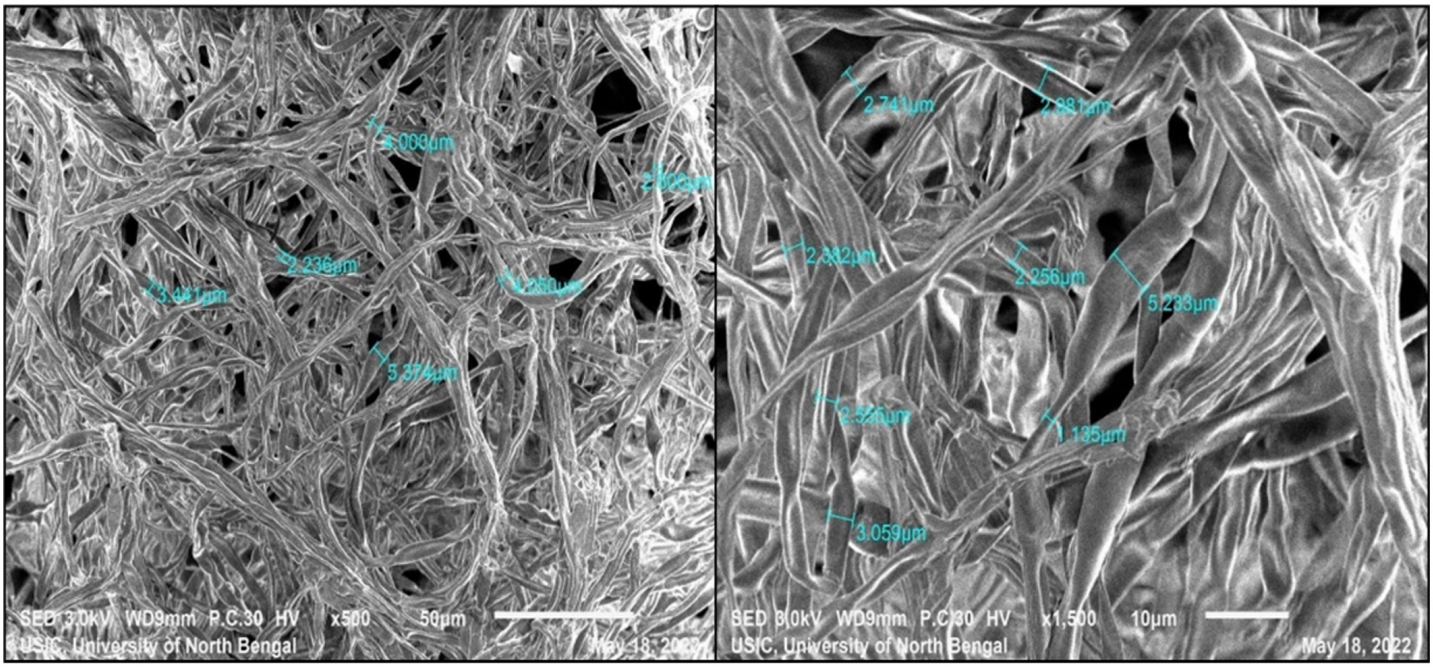
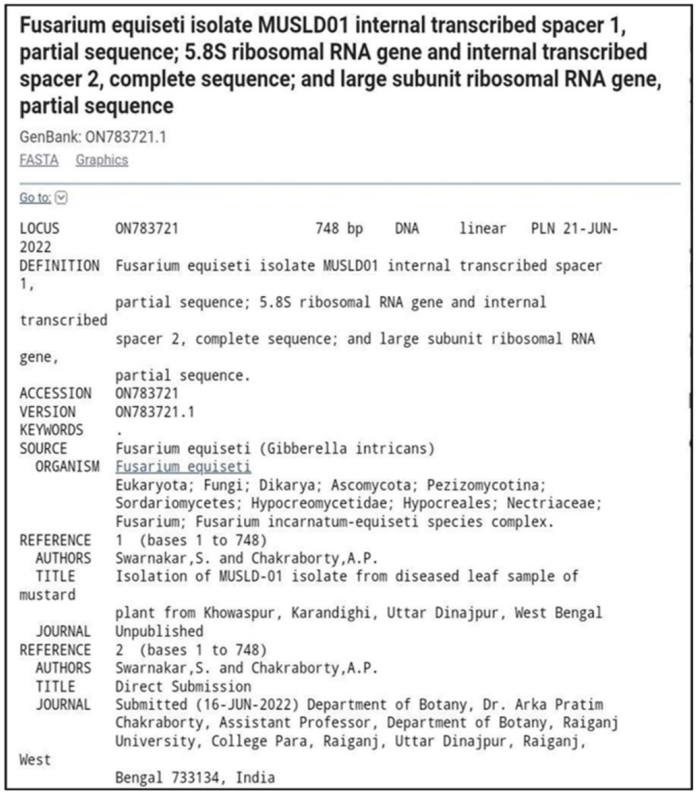


Figure 3

Light microscopic and scanning electron microscopic (SEM) observations of MUSLD-01 showing characteristic mycelial and conidial structures of Fusarium equiseti.



Fusarium equiseti isolate MUSLD01 internal transcribed spacer 1, partial sequence; 5.8S ribosomal RNA gene and internal transcribed spacer 2, complete sequence; and large subunit ribosomal RNA gene, partial sequence

GenBank: ON783721.1

FASTA Graphics

Go to:

```
LOCUS       ON783721                748 bp    DNA     linear   PLN 21-JUN-
2022
DEFINITION  Fusarium equiseti isolate MUSLD01 internal transcribed spacer
1,
            partial sequence; 5.8S ribosomal RNA gene and internal
transcribed
            spacer 2, complete sequence; and large subunit ribosomal RNA
gene,
            partial sequence.
ACCESSION   ON783721
VERSION     ON783721.1
KEYWORDS    .
SOURCE      Fusarium equiseti (Gibberella intricans)
  ORGANISM  Fusarium equiseti
            Eukaryota; Fungi; Dikarya; Ascomycota; Pezizomycotina;
            Sordariomycetes; Hypocreomycetidae; Hypocreales; Nectriaceae;
            Fusarium; Fusarium incarnatum-equiseti species complex.
REFERENCE   1  (bases 1 to 748)
  AUTHORS   Swarnakar,S. and Chakraborty,A.P.
  TITLE     Isolation of MUSLD-01 isolate from diseased leaf sample of
mustard
            plant from Khowaspur, Karandighi, Uttar Dinajpur, West Bengal
  JOURNAL   Unpublished
REFERENCE   2  (bases 1 to 748)
  AUTHORS   Swarnakar,S. and Chakraborty,A.P.
  TITLE     Direct Submission
  JOURNAL   Submitted (16-JUN-2022) Department of Botany, Dr. Arka Pratim
            Chakraborty, Assistant Professor, Department of Botany, Raiganj
            University, College Para, Raiganj, Uttar Dinajpur, Raiganj,
West
            Bengal 733134, India
```

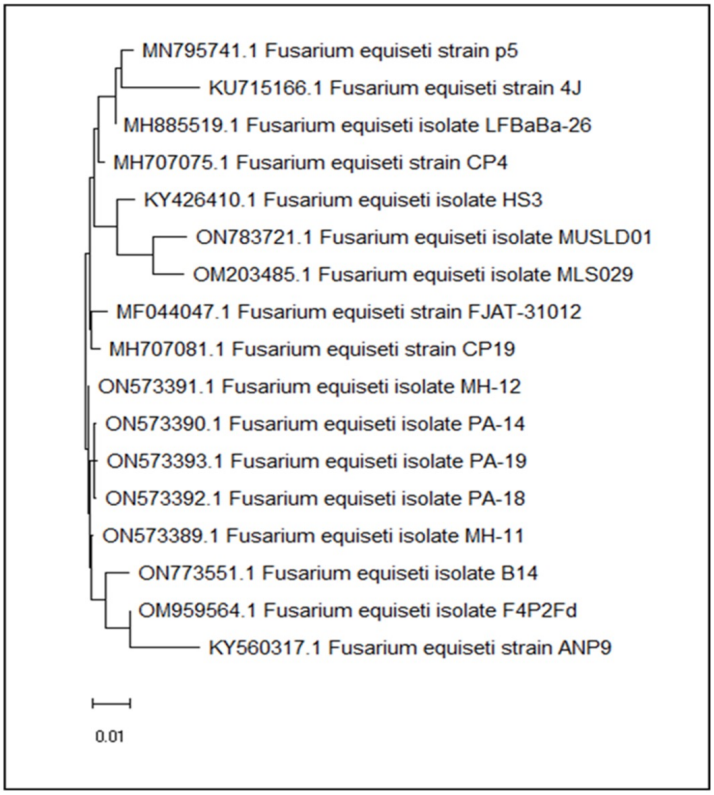


Figure 4

Molecular identification of MUSLD-01 isolate based on 5.8S rDNA sequencing confirming Fusarium equiseti (GenBank accession no. ON783721).

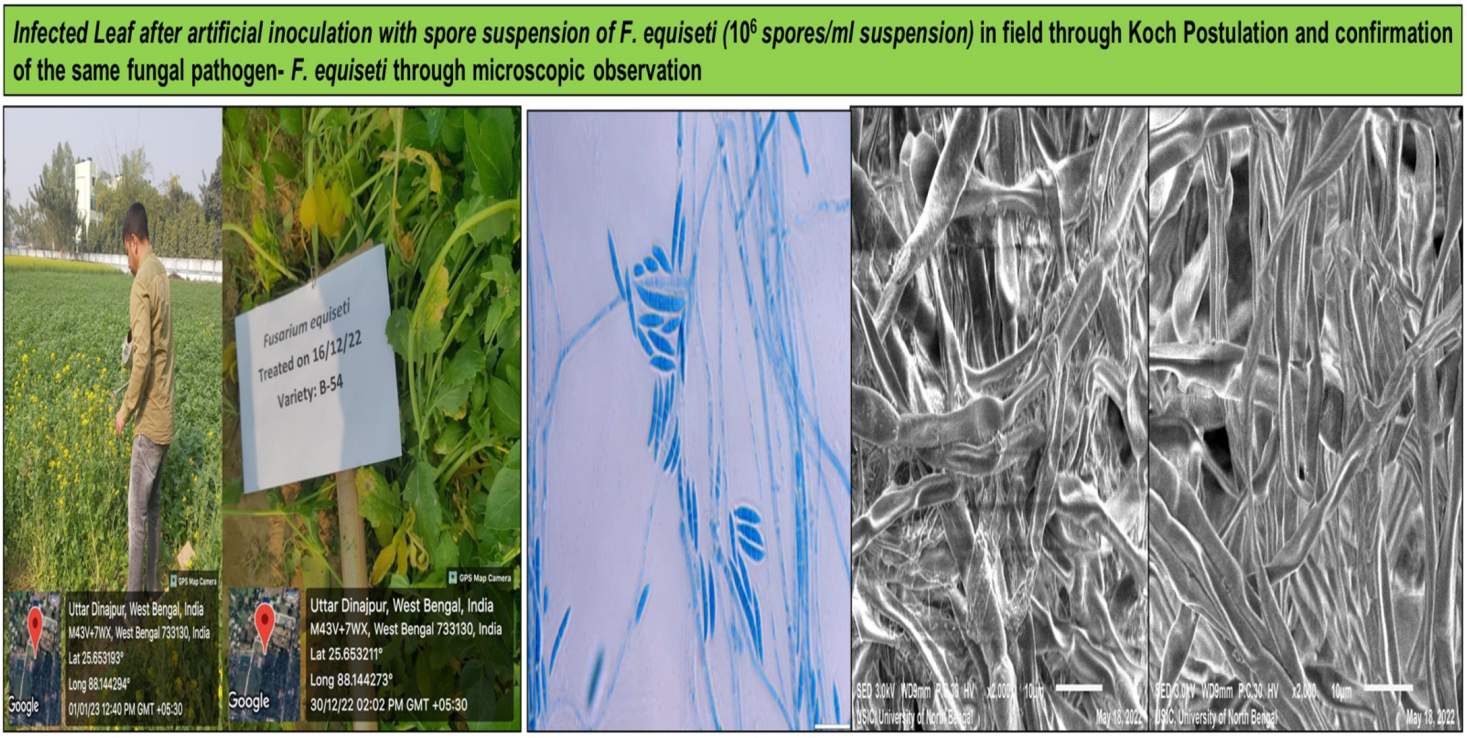


Figure 5

Artificial inoculation of Fusarium equiseti spores (10^6 spores ml^{-1}) on healthy mustard plants and re-isolation of the pathogen, fulfilling Koch's postulates.

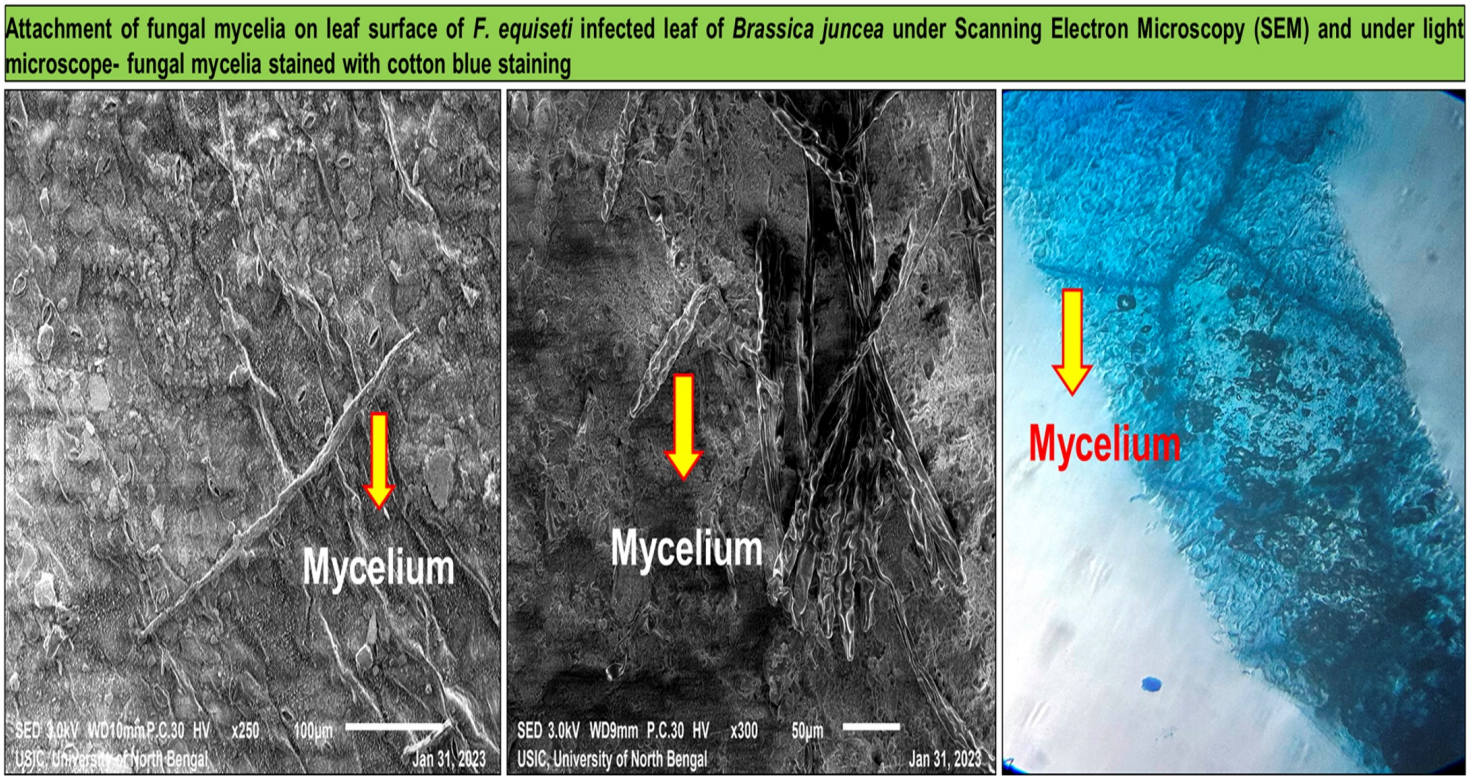


Figure 6

SEM images showing attachment and colonization of Fusarium equiseti mycelia on the leaf surface of infected Brassica juncea plants.

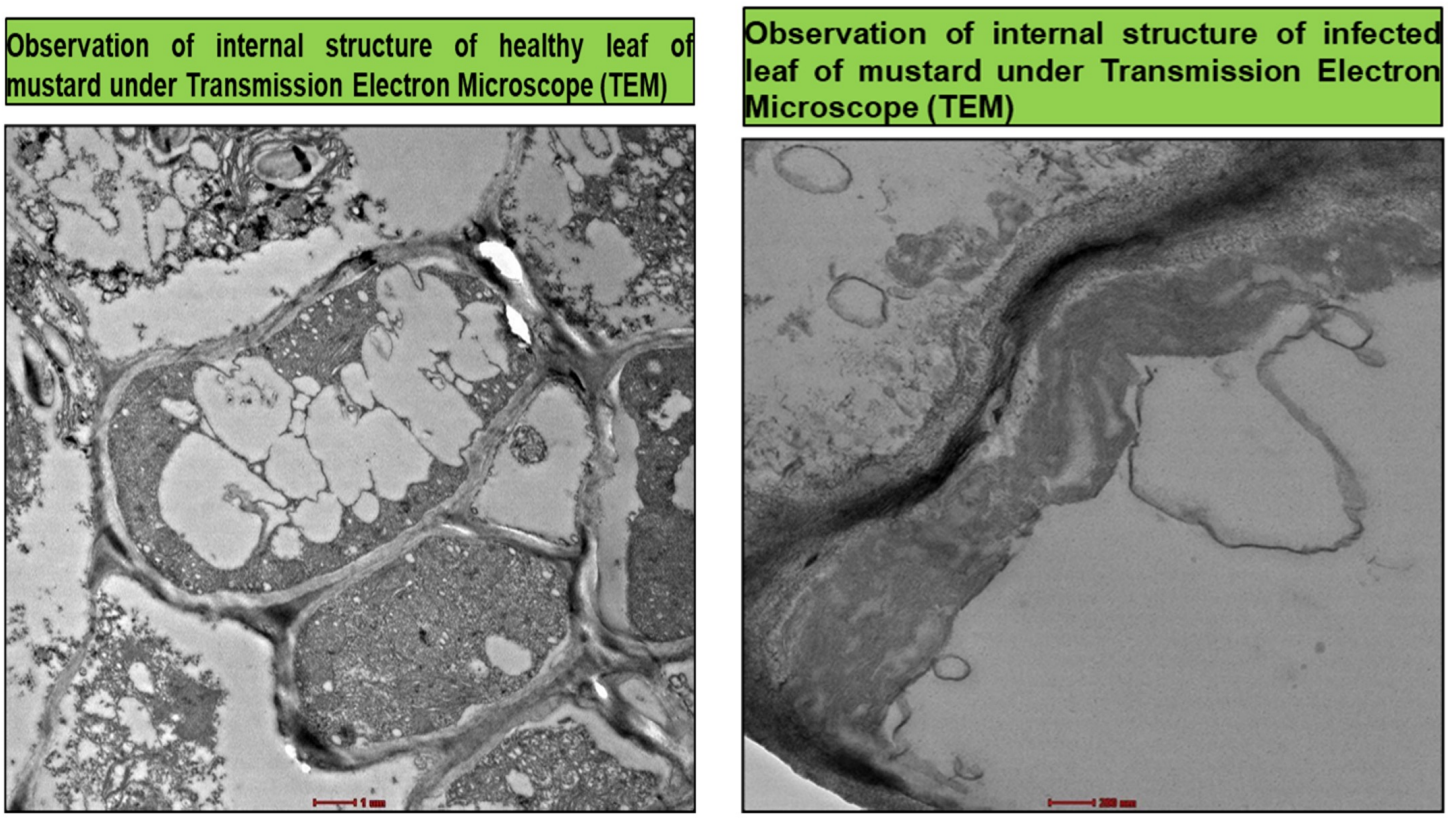


Figure 7

Transmission electron microscopy (TEM) images showing internal leaf ultrastructure of (a) healthy mustard leaf and (b) F. equiseti-infected leaf, indicating cellular disorganization in infected tissues.

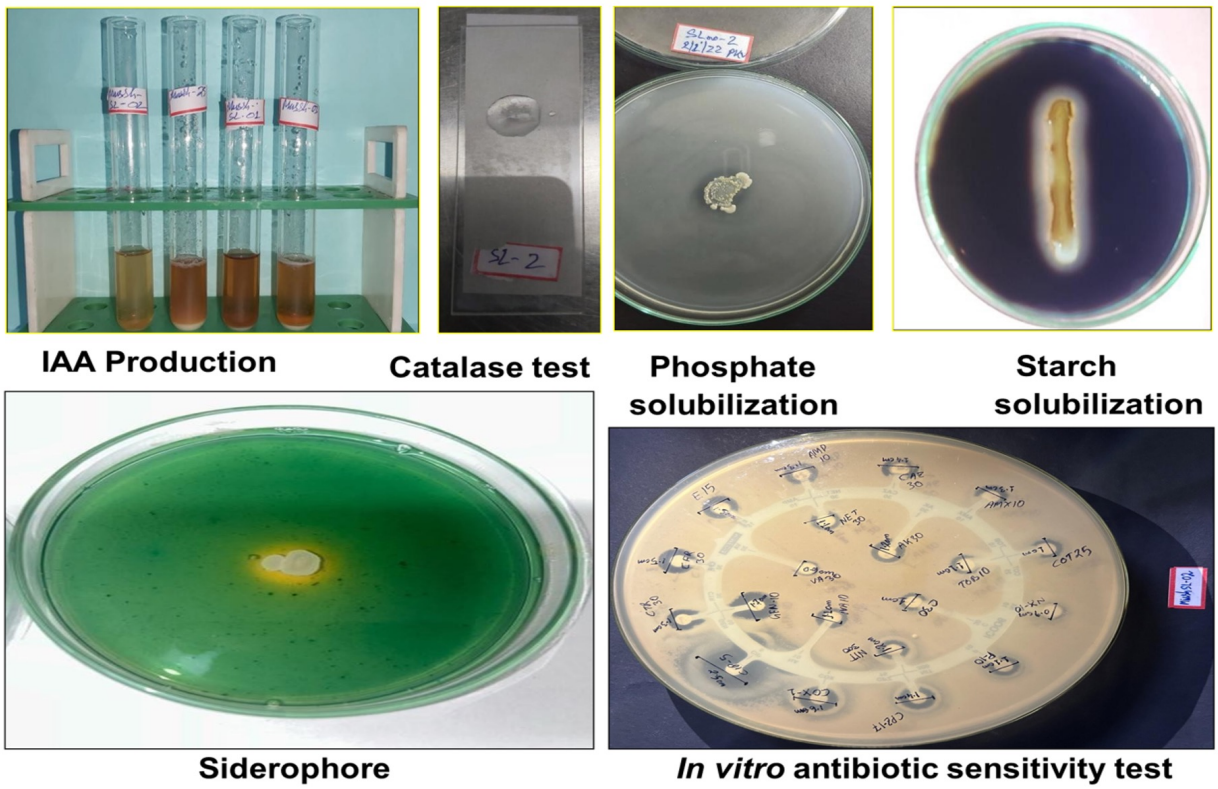


Figure 8

Isolation and screening of plant growth–promoting rhizobacteria (PGPR) from mustard rhizospheric soil showing positive reactions for IAA production, phosphate solubilization, siderophore production, and catalase activity.

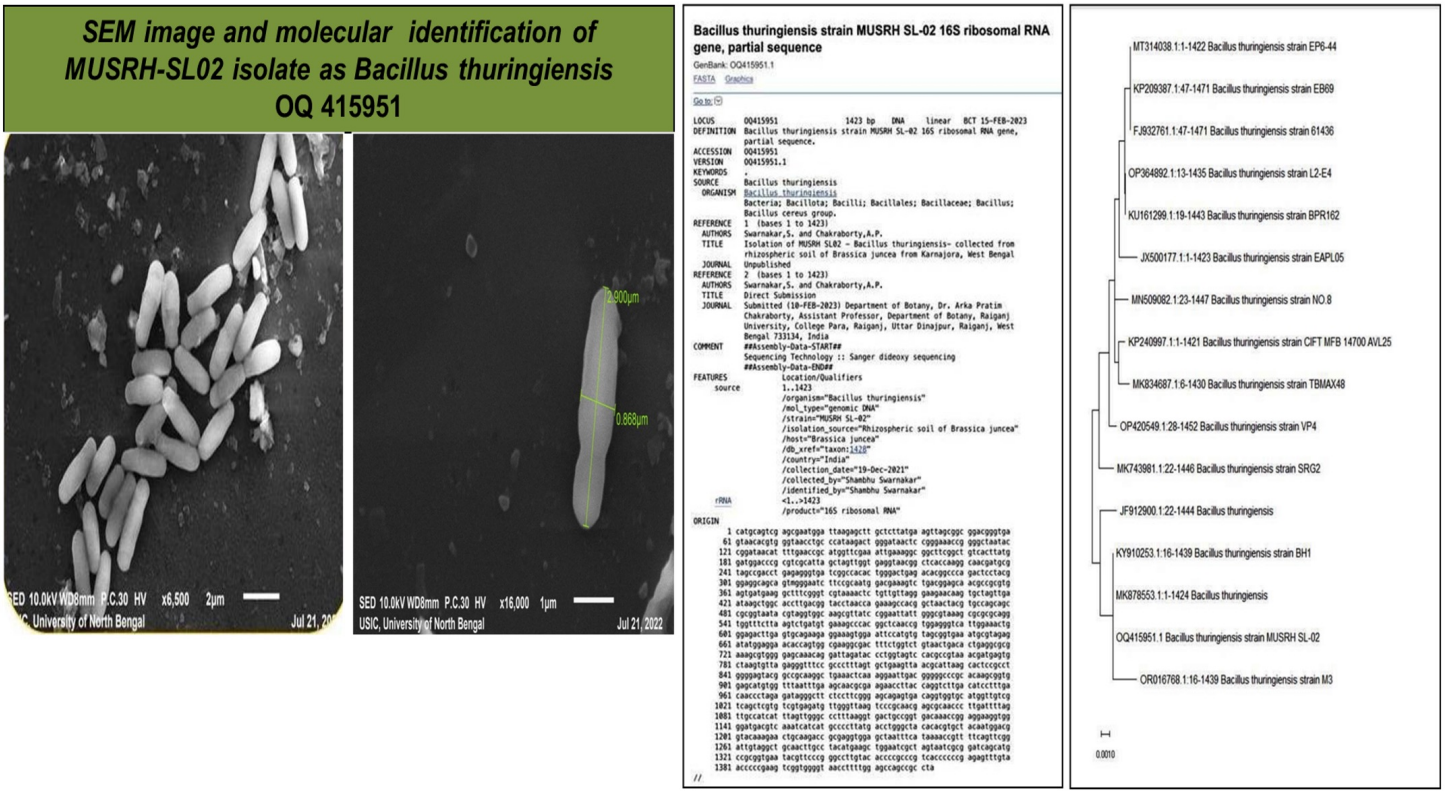


Figure 9

SEM images and molecular identification of PGPR isolates:

(a) Bacillus thuringiensis (OQ415951) and

(b) Bacillus pumilus (ON783696).

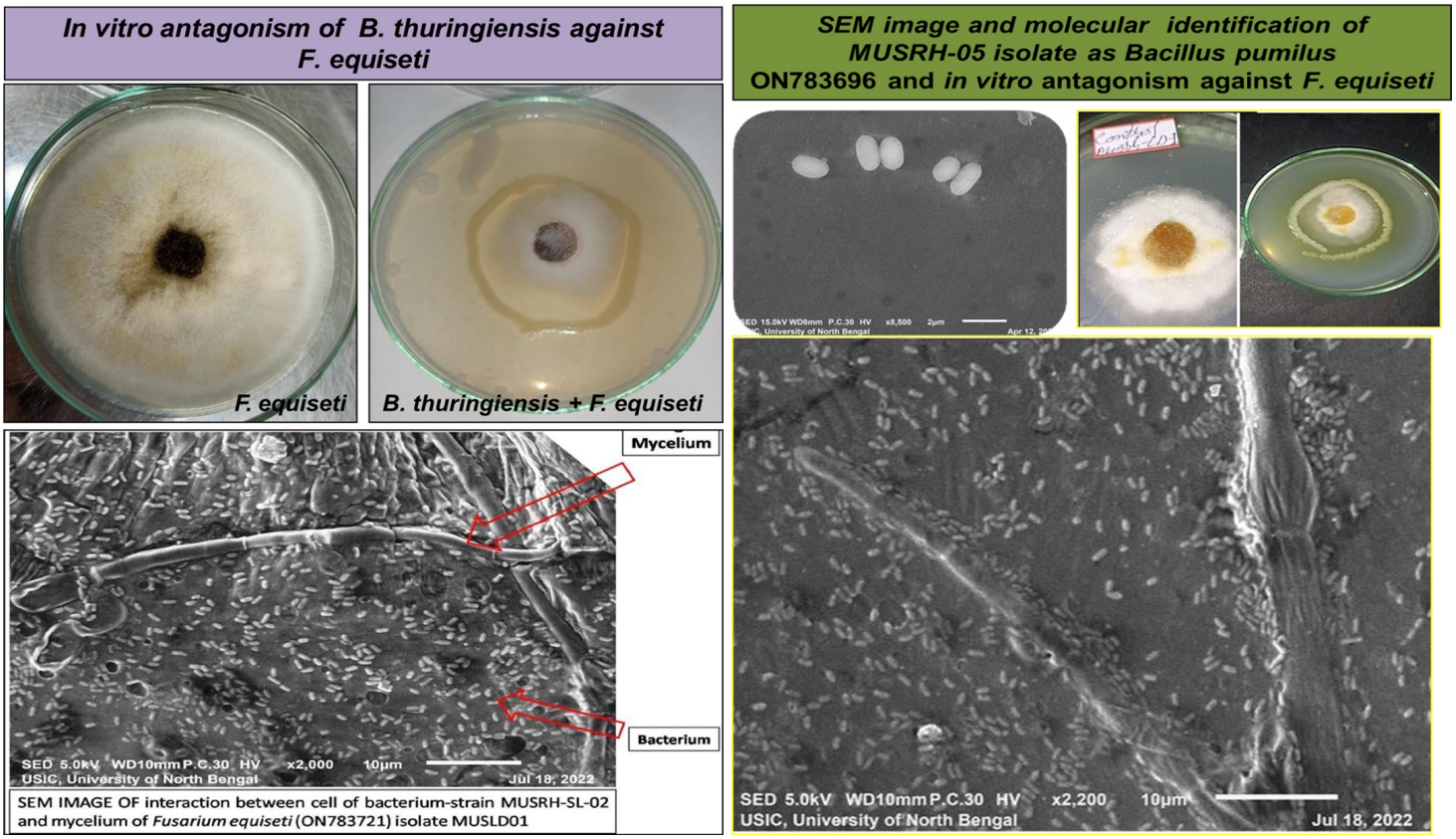
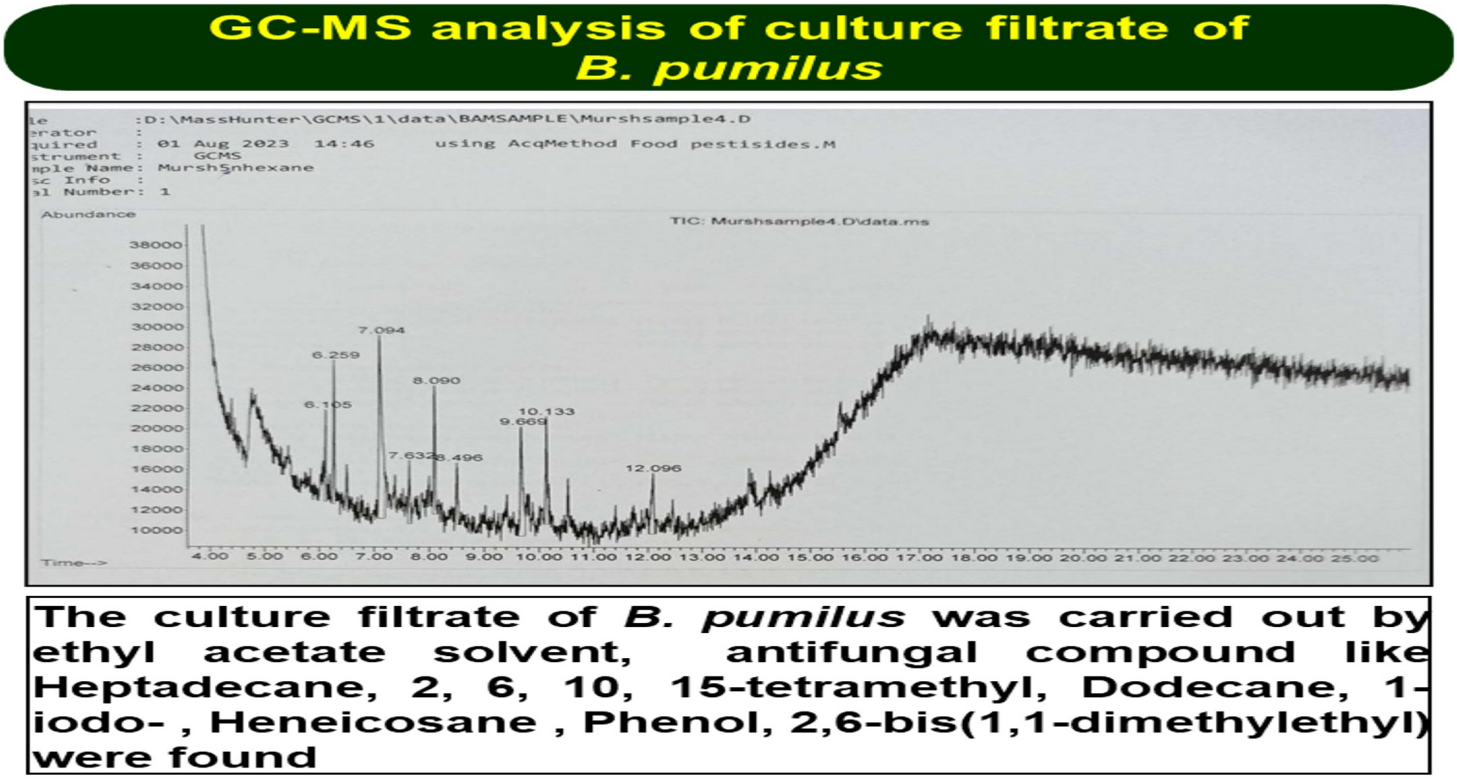


Figure 10

In vitro antagonistic activity of Bacillus thuringiensis and Bacillus pumilus against Fusarium equiseti in dual culture assay on PDA medium.



The culture filtrate of *B. pumilus* was carried out by ethyl acetate solvent, antifungal compound like Heptadecane, 2, 6, 10, 15-tetramethyl, Dodecane, 1-iodo- , Heneicosane , Phenol, 2,6-bis(1,1-dimethylethyl) were found

Figure 11

GC–MS chromatogram of ethyl acetate extract of culture filtrate of Bacillus thuringiensis showing presence of bioactive antifungal metabolites.

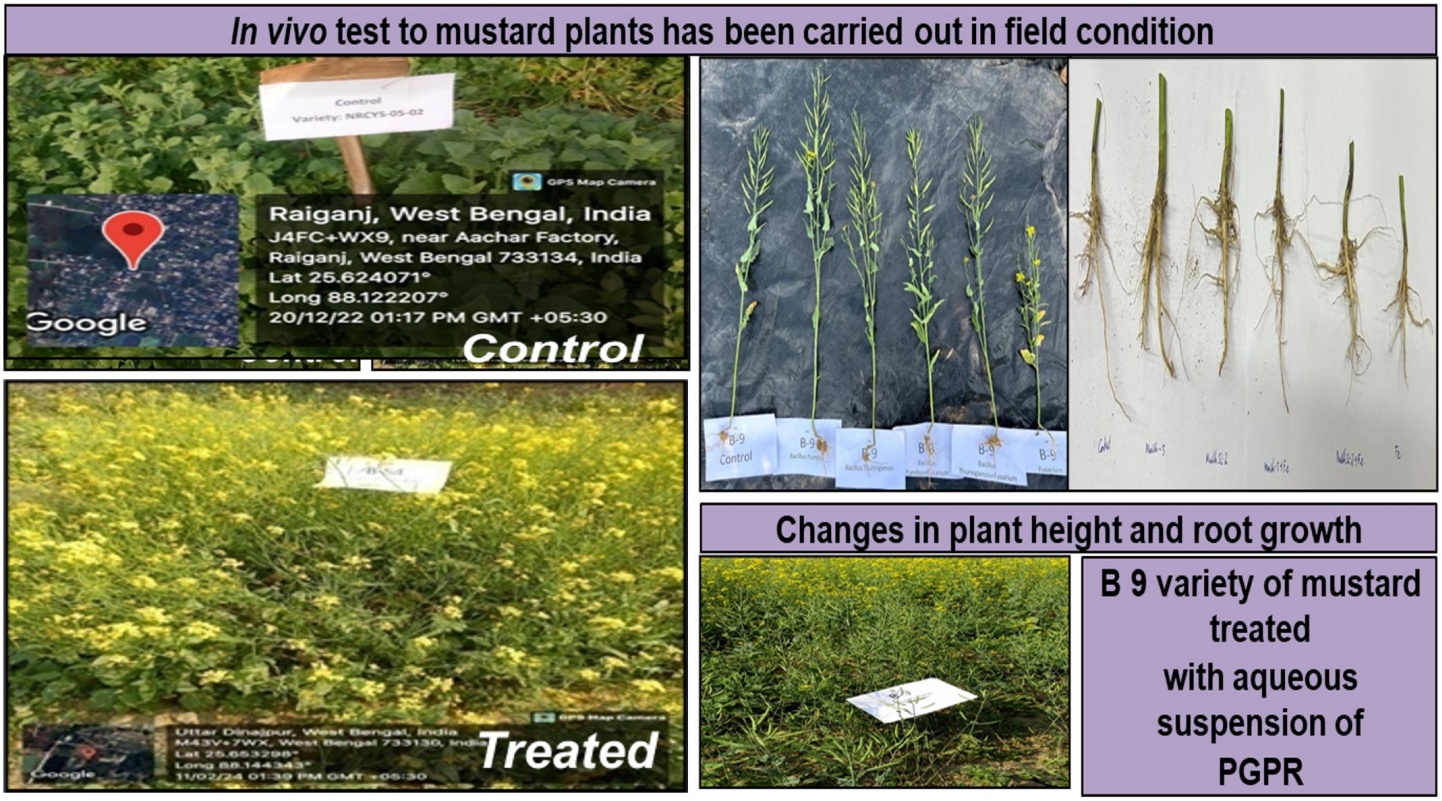


Figure 12

GC–MS chromatogram of ethyl acetate extract of culture filtrate of Bacillus pumilus indicating antifungal compounds such as heptadecane, phenolic derivatives, and long-chain hydrocarbons.



Figure 13

Field evaluation of mustard plants under different treatments:

Control, PGPR-treated, F. equiseti-inoculated, and PGPR + F. equiseti-treated plants showing reduced disease severity and improved growth.

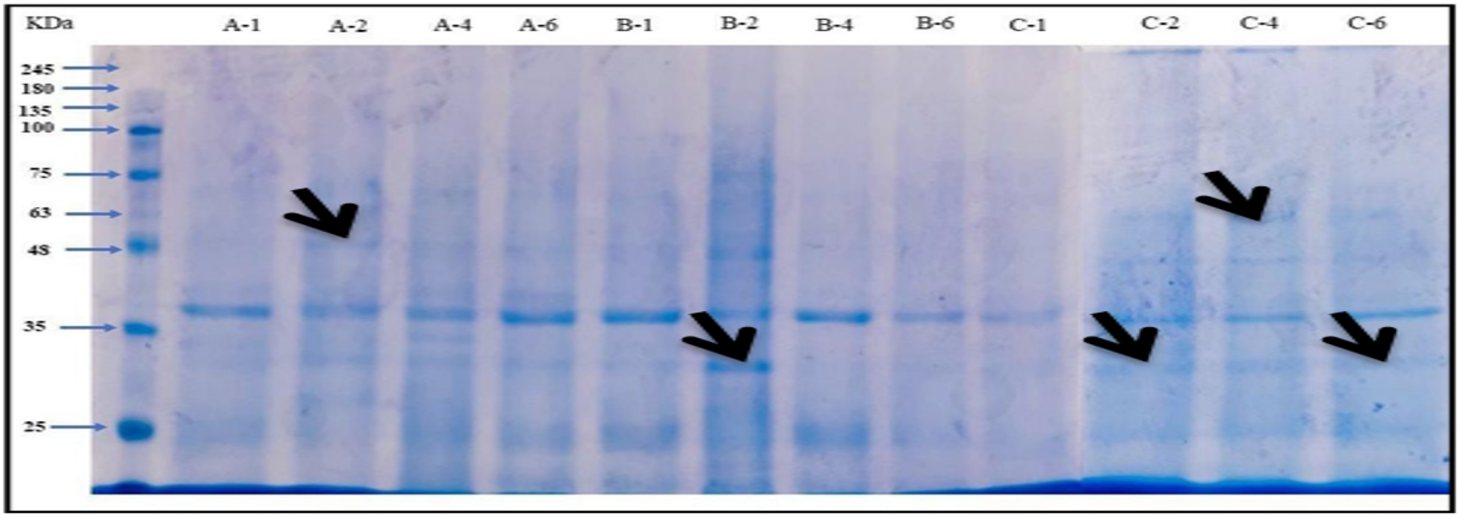


Figure 14

Effect of PGPR application on plant growth parameters (plant height and root length) of mustard varieties under field conditions.

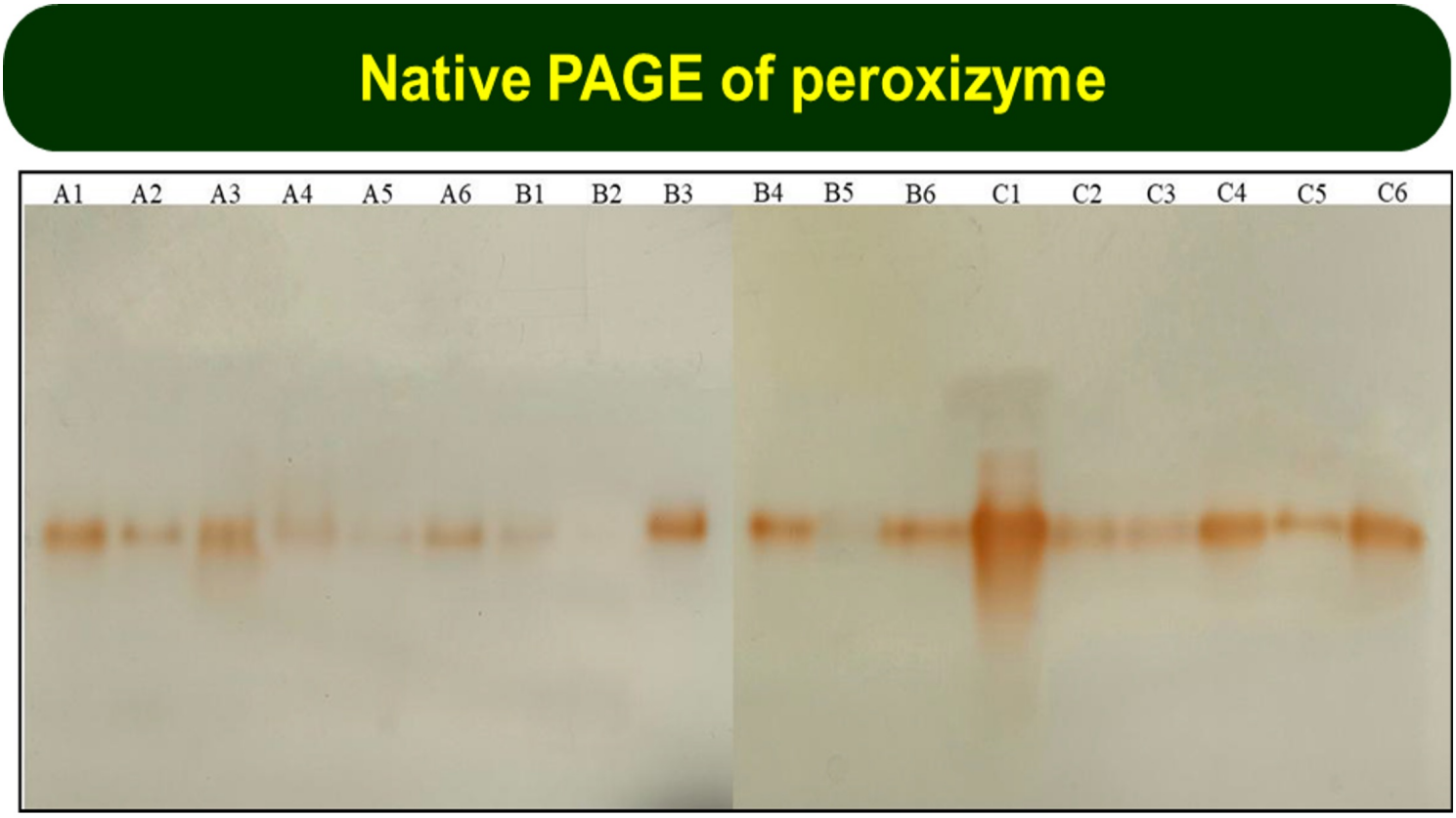


Figure 15

SDS-PAGE analysis showing variation in total protein profiles of mustard plants under different treatments.